

THESIS FOR THE DEGREE OF DOCTOR OF PHILOSOPHY

**Understanding overlooked molecular  
interactions in the cellulose/NaOH(aq)  
system**

MARIA GUNNARSSON

*Department of Chemistry and Chemical Engineering*

CHALMERS UNIVERSITY OF TECHNOLOGY

Göteborg, Sweden 2019

# Understanding overlooked molecular interactions in the cellulose/NaOH(aq) system

MARIA GUNNARSSON

ISBN 978-91-7905-172-3

© Maria Gunnarsson, 2019

Doktorsavhandlingar vid Chalmers tekniska högskola

Ny serie nr 4639

ISSN 0346-718X

Chalmers University of Technology

Department of Chemistry and Chemical Engineering

SE-412 96 Göteborg, Sweden

Phone: +46 (0)31-772 10 00

## **Cover:**

Schematic representation of cellulose in NaOH(aq) with additives entering a radio-frequency coil in a magnetic field, recording a spectrum. Illustration made by Diana Bernin and Jenny Bengtsson.

Printed by Chalmers Reproservice

Göteborg, Sweden 2019

# Understanding overlooked molecular interactions in the cellulose/NaOH(aq) system

MARIA GUNNARSSON

Department of Chemistry and Chemical Engineering  
Chalmers University of Technology

## Abstract

The cold NaOH(aq) system is a promising process for the production of textile fibres. Although the process has been studied for almost a century, there remain unsolved research issues, especially regarding the dissolution mechanism. The focus of the thesis is to investigate the fundamental molecular interactions that govern the behaviour of a pure cellulose/NaOH(aq) system and systems containing selected additives. Nuclear magnetic resonance (NMR) spectroscopy in combination with complementary methods, such as infrared spectroscopy and pH, was used as characterisation technique, including substantial work on method development.

The main findings of the thesis show that magnetisation transfer NMR has great potential for studying the dynamics of water exchange in a cellulose/aqueous alkali system, which gives valuable insights into the dissolution mechanism of cellulose in NaOH(aq). Evaluation of  $^3J_{\text{HH}}$  and  $^1J_{\text{CH}}$  couplings of the cellulose model compound methyl  $\beta$ -D-glucopyranoside ( $\beta$ -MeO-Glcp) showed that conformational changes occur in NaOH(aq), but not as a function of temperature. However, upon the addition of urea, temperature-dependent conformational changes were observed. Steady-state heteronuclear Overhauser effect NMR measurements confirmed a non-specific interaction between urea and cellulose. This non-specific interaction suggests that urea facilitates a chemical environment that promotes a conformational change in the  $\beta$ -MeO-Glcp, which is most likely one of the mechanisms behind the positive effect of urea on the dissolution of cellulose in NaOH(aq).  $\text{CO}_2$  from the surrounding air was found to dissolve readily in cellulose/NaOH(aq) solutions, which leads to the formation of a cellulose carbonate intermediate and the introduction of substantial  $\text{CO}_3^{2-}$  that is capable of interacting with cellulose. Cellulose- $\text{CO}_3^{2-}$  interactions were found to be disrupted in the presence of urea in NaOH(aq). Taken together, it is suggested that the cellulose- $\text{CO}_3^{2-}$  interactions are one of the factors that promote gelling. Urea is likely able to delay gelation due to the disruption of cellulose- $\text{CO}_3^{2-}$  interactions. The discovery of carbonate chemistry in cellulose/NaOH(aq) solutions reveals a new dimension of these solutions with high relevance for the stability and implementation of the cold NaOH(aq) process.

**Keywords:** cellulose, dissolution, NaOH(aq),  $\text{CO}_2$ , urea, NMR, ATR-IR





*Till alla kvinnor som gjorde detta möjligt*



# List of publications

This thesis is based on the following publications:

- I **Maria Gunnarsson**, Hans Theliander and Merima Hasani  
“Chemisorption of air CO<sub>2</sub> on cellulose: an overlooked feature of the cellulose/NaOH(aq) dissolution system” in *Cellulose*, Volume 24, Issue 6, 2017, pp.2427-2436.
- II **Maria Gunnarsson**, Diana Bernin, Åsa Östlund and Merima Hasani  
“The CO<sub>2</sub> capturing ability of cellulose dissolved in NaOH(aq) at low temperature” in *Green Chemistry*, Volume 20, Issue 14, 2018, pp.3279-3286.
- III **Maria Gunnarsson**, Diana Bernin and Merima Hasani  
“The CO<sub>2</sub>/CO<sub>3</sub><sup>2-</sup> chemistry of the NaOH(aq) model system applicable to cellulose solutions” *Submitted to Cellulose*.
- IV **Maria Gunnarsson**, Diana Bernin and Merima Hasani  
“Capturing of CO<sub>2</sub> in NaOH(aq) in the presence of urea and methyl β-D-glucopyranoside” *Submitted to Advanced Sustainable Systems*.
- V **Maria Gunnarsson**, Merima Hasani and Diana Bernin  
“Influence of urea on methyl β-D-glucopyranoside in alkali at different temperatures” *Accepted to Cellulose*.
- VI **Maria Gunnarsson**, Merima Hasani and Diana Bernin  
“The potential of magnetisation transfer NMR to monitor the dissolution process of cellulose in cold alkali” *Accepted to Cellulose*.

# Contribution report

The author of this thesis has made the following contributions to the publications included:

- I Main author. Contributed to the formulation of the research problem, planned and performed the experimental work. Analysed and interpreted the results and wrote the publication with support from the co-authors.
- II Main author. Contributed to the formulation of the research problem, planned and performed the experimental work. Analysed and interpreted the results and wrote the publication with support from the co-authors.
- III Main author. Contributed to the formulation of the research problem, planned and performed the experimental work. Analysed and interpreted the results and wrote the publication with support from the co-authors.
- IV Main author. Contributed to the formulation of the research problem, planned and performed the experimental work. Analysed and interpreted the results and wrote the publication with support from the co-authors.
- V Main author. Contributed to the formulation of the research problem, planned and performed the experimental work. Analysed and interpreted the results and wrote the publication with support from the co-authors.
- VI Contributed to the formulation of the research problem and performed half of the experimental work. Contributed to the analysis, interpretation of the results, and writing of the manuscript.

Part of this work has been presented by the author at:

**14<sup>th</sup> European Workshop on Lignocellulosics and Pulp**

28 – 30 June 2016, *Grenoble, France*, (poster presentation).

**5<sup>th</sup> Avancell conference**

18 – 19 October 2016, *Göteborg, Sweden*, (oral presentation).

**5<sup>th</sup> EPNOE International Polysaccharide Conference**

20 – 24 August 2017, *Jena, Germany*, (oral presentation).

**15<sup>th</sup> European Workshop on Lignocellulosics and Pulp**

26 – 29 June 2018, *Aveiro, Portugal*, (poster presentation).

**8<sup>th</sup> Workshop on Cellulose, Regenerated cellulose and Cellulose derivatives**

13 – 14 November 2018, *Karlstad, Sweden*, (oral presentation).

**Ekmandagarna**

29 – 30 January 2019, *Stockholm, Sweden*, (oral presentation).

## List of abbreviations

$\alpha$ -MeO-Glcp	methyl $\alpha$ -D-glycopyranoside
$\beta$ -MeO-Glcp	methyl $\beta$ -D-glycopyranoside
AGU	anhydroglucosidic unit
ATR-FTIR	attenuated total reflectance Fourier transform infrared spectroscopy
BMIMCl	1-butyl-3-methylimidazolium chloride
CSC	cellulose synthesis complex
DMF	dimethylformamide
DS	degree of substitution
DP	degree of polymerisation
DMSO	dimethylsulfoxide
EMIMAc	1-ethyl-3-methylimidazole acetate
FID	free induction decay
<i>gg</i>	gauche-gauche
<i>gt</i>	gauche-trans
HOE	heteronuclear Overhauser effect
HSQC	heteronuclear single quantum coherence
MT	magnetisation transfer
MCC	microcrystalline cellulose
MeOH	methanol
NMMO	N-methylmorpholine N-oxide
NMR	nuclear magnetic resonance
NOE	nuclear Overhauser effect
<i>tg</i>	trans-gauche
ZnO	zinc oxide

# Table of Contents

<b>1</b>	<b>Introduction</b>	<b>1</b>
1.1	Background . . . . .	2
1.2	Objective . . . . .	3
<b>2</b>	<b>Cellulose</b>	<b>5</b>
2.1	Cellulose structure and morphology . . . . .	6
2.2	Cellulose solubility . . . . .	9
<b>3</b>	<b>The cold NaOH(aq) solvent system</b>	<b>15</b>
3.1	Fundamentals of the NaOH(aq) cellulose dissolution system . . . .	16
3.2	Impact of additives on dissolution in NaOH(aq) . . . . .	19
3.3	Analytical challenges of the cellulose/NaOH(aq) system . . . . .	21
<b>4</b>	<b>Methodology for understanding the molecular dimension of the cellulose/NaOH(aq) system and its controversies</b>	<b>23</b>
4.1	Investigating and understanding controversies of the cellulose/NaOH(aq) system . . . . .	24
4.2	Analytical tools and experimental setups . . . . .	24
<b>5</b>	<b>Driving forces for dissolution of cellulose in aqueous alkalis</b>	<b>31</b>
5.1	Cellulose dissolution capacity of different aqueous alkalis as a function of temperature . . . . .	32
5.2	Relaxation rates of H <sub>2</sub> O and MCC in different aqueous alkalis at increasing temperature . . . . .	34
5.3	Magnetisation transfer as a tool for monitoring swelling of cellulose	36
<b>6</b>	<b>Conformational changes promoting dissolution</b>	<b>41</b>
6.1	Solvent effects on $J_{HH}$ coupling values . . . . .	42
6.2	Temperature effects on chemical shifts and $^1J_{CH}$ coupling values . .	44
6.3	Association of urea with a cellulose model compound . . . . .	47

<b>7</b>	<b>Molecular interactions in relation to CO<sub>2</sub> uptake in NaOH(aq)</b>	<b>51</b>
7.1	Influence on the chemical environment in NaOH(aq) by the addition of CO <sub>2</sub> . . . . .	52
7.2	pH variation of NaOH(aq) induced by addition of different solutes .	55
7.3	Catalytical capture of CO <sub>2</sub> in NaOH(aq) by MeO-Glcp and urea . . .	57
7.4	Is there association between CO <sub>3</sub> <sup>2-</sup> and cellulose? . . . . .	60
<b>8</b>	<b>Conclusions</b>	<b>65</b>
<b>9</b>	<b>Outlook</b>	<b>69</b>



# 1

## Introduction

*In this chapter, the subject of the thesis is described through a brief background description of the field, its history, and its existing industrial and scientific challenges. The objective for the thesis, which was the foundation for the scientific work performed, is presented and framed from scientific controversies of the field.*

## 1.1 Background

While the Earth's population continues to grow, reaching nearly 7.4 billion people during 2019, the need for products used in the daily life is also expanding. One of those products is clothes. This is reflected in the consumption of textile fibre, which increased from 78 million tons to more than 103 million during the last decade.<sup>1</sup> The majority of textile fibres produced today use fossil oil as a raw material. Fossil oil is a finite resource and, therefore, associated with environmental issues. For this reason, the raw material for textile fibres needs to be replaced with renewable resources. However, a renewable resource is not necessarily a sustainable resource. Cotton, for example, has been used for textile fibres for thousands of years and originates from a natural and renewable resource, but its production has been questioned from a sustainability point of view due to its use of arable land, massive demand for water, and use of pesticides during cultivation.<sup>2,3</sup>

As an alternative to cotton, cellulose derived from wood is an interesting feedstock, but it entails additional processing to reach a textile fibre product. Unlike cotton, cellulose fibres derived from wood are short and wide with rather stiff morphology and, therefore, demand re-shaping into long and thin fibres that are possible to spin into a yarn. The re-shaping is typically done through the dissolution of the cellulose in a solvent, followed by precipitation and then washing in a spin bath containing an anti-solvent. Only a few such processes, with the most common ones being the viscose and the lyocell processes, have been commercialised mainly because of difficulties with finding suitable solvents for the dissolution step. The reason for this is the complexity of the cellulose morphology and supramolecular organisation, which inhibit dissolution in common solvents. The fibre properties in combination with the environmental footprint from the viscose process is one of the reasons why the development of appropriate and sustainable dissolution processes continues to be an important issue.

One of the most attractive solvent systems, both in terms of sustainability and commercial implementation, is the cold NaOH(aq) system. The system is considered to have a low environmental burden due to the fact that it is water-based and that there is already an existing infrastructure for the recycling and handling of NaOH, which is currently used as a process chemical in pulp and paper mills. A simple integration of a dissolution process that utilises NaOH(aq) as a solvent into an existing pulp mill to convert cellulose fibres to textile fibres

is, therefore, feasible. Nevertheless, this solvent system has its peculiarities. Cellulose only dissolves at low temperature and within a narrow concentration of NaOH. Moreover, the obtained solutions are not stable during both dissolution and subsequent handling, which is an obstacle for large scale implementation of the process. In order to overcome these obstacles and reach industrial implementation, that is economically and environmentally viable, it is essential to understand the true dissolution mechanism for cellulose in this particular solvent system.

A lot of effort has been put into addressing these issues, which has resulted in a number of theories on the driving forces behind the dissolution of cellulose in NaOH(aq).<sup>4</sup> In addition to this, additives used to improve the dissolution capacity of the solvent, such as urea, are described in various ways to act either on the solvent system or on the cellulose, but no definite explanation for their role in the dissolution mechanism has been concretised.

## 1.2 Objective

The objective of this thesis is to increase knowledge on overlooked features of the NaOH(aq) solvent system important to the understanding of cellulose dissolution. These overlooked features include the inherent ability of NaOH(aq) to dissolve and convert  $\text{CO}_2$  to  $\text{CO}_3^{2-}$ , the conformational changes that occur in a cellulose molecule due to the addition of urea and variation in temperature when dissolved in NaOH(aq), and the variation in cellulose swelling and water dynamics in different aqueous alkali hydroxides.

The aim, using a variety of NMR spectroscopic methods, is to elucidate on the particular molecular interactions that occur in a system of NaOH(aq) and dissolved cellulose or a cellulose model compound in the presence of selected additives and upon temperature variations. The reason for this aim is to gain valuable insight into the interactions of a system that could be implemented in a process on a commercial scale.



# 2

## Cellulose

*Cellulose is the most abundant polymer in nature, and is together with hemicellulose and lignin one of the main components of wood. The three constituents coexist in a complex matrix but can be separated by specific chemicals, which allows them to be used more effectively in different types of applications. This is the concept of a wood-based biorefinery, where all building blocks are utilised for their best purpose before energy recovery is considered. Cellulose, as such, can be re-shaped into a variety of products such as textile fibres, membranes and barriers. This chapter describes the structure and morphology of cellulose, and the challenges that are faced in dissolving cellulose.*

## 2.1 Cellulose structure and morphology

The cellulose polymer is a carbohydrate that consists of D-glucopyranose units, also called anhydroglucosidic units (AGU), linked together through a  $\beta$ -1,4-glycosidic bond, as shown in Figure 2.1.<sup>5</sup> The polymer is synthesised through a six-lobed rosette cellulose synthesis complex (CSC) located at, or outside, the plasma membrane from which the cellulose chains are extracted.<sup>6</sup> Each lobe of the CSC is suggested to contain three sites that extrude one chain each, which results in 18 chains synthesised from one CSC.<sup>7,8</sup> The three equatorially positioned hydroxyl groups of each AGU enable hydrogen bonding both intramolecularly between hydroxyl groups within the same chain and intermolecularly between hydroxyl groups on neighbouring chains. The former stabilises a flat chain conformation, while the latter leads to the alignment of the cellulose chains next to each other, forming a sheet-like structure. Stacking then occurs due to additional forces between the sheets, which gives cellulose a crystalline and, subsequently, a microfibrillar structure.

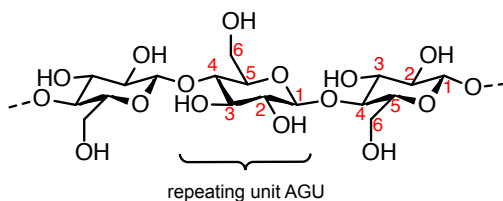


**Figure 2.1:** The molecular structure of cellulose. Each position is numbered in the repeating AGU unit.

The sheet stacking is suggested to occur due to several reasons. One being that the  $^4C_1$  chair conformation (which describes the C4 position being located above the C1 position in the ring), and the equatorial position of the hydroxyl groups provides an optimal configuration for a multiplicity of C-H $\cdots$ O hydrogen bonds from one sheet to the next.<sup>9</sup> Another suggestion is that hydrophobic interactions between the glucose ring surfaces, which gives cellulose an amphiphilic character, cause association between the sheets.<sup>10</sup> The cellulose structure is, however, not fully crystalline but contains less ordered regions said to originate from a kink occurring every 6-7 AGU, which results in both ordered and less ordered regions in the structure. The kink, which occurs on the molecular level, develops into a twist that emerges throughout

the macromolecular structure and contributes to the final geometry of the microfibril. Lastly, semicrystalline microfibrils are aggregated into macrofibrils, which in turn, are deposited in different layers of the cell walls, thus forming the cellulose part of a fibre. The cellulose is embedded in a matrix with lignin, which is regarded as the glue between the fibres, and hemicelluloses, which provides interactions between the cellulose and lignin, and together forms the wood material (Figure 2.2).

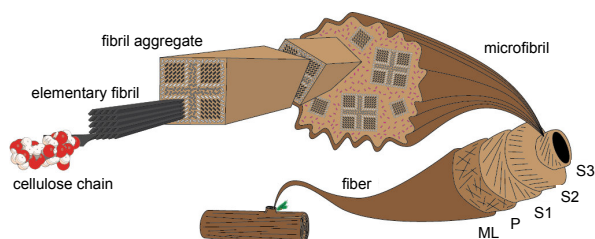


**Figure 2.2:** *The morphology of cellulose derived from wood. Adapted with permission from A. Idström.*

The length of a cellulose chain is defined by the number of AGUs, which means the degree of polymerisation (DP). The DP of cellulose originating from wood is estimated to be between 9,000 and 10,000. During pulping, hemicelluloses and lignin are largely removed, while the cellulose is preserved as much as possible. The DP of the cellulose will, however, decrease to 300-1,700 depending on the type of pulping process used. Cellulose in wood fibres to be used for the production of textile fibres has a typical DP of 250 to 600 and is termed dissolving pulp.<sup>11</sup>

It is evident that the conformation of the cellulose monomeric unit plays a crucial role in the preferred association that takes place between the chains on a macromolecular level and affects the resulting properties of the cellulose fibre. This is a feature also observable for the different allomorphs of cellulose that are present naturally and obtained upon treatment. The crystalline structure of cellulose is, in general, highly influenced by the conformation of the hydroxymethyl group (primary alcohol) on the cellulose, which can be seen as a change in the hydrogen bonding pattern. Depicted in Figure 2.3 are the three staggered conformations suggested for the hydroxymethyl group: gauche-gauche (gg,  $\omega=$

-60°), gauche-trans (*gt*,  $\omega = 60^\circ$ ) and trans-gauche (*tg*,  $\omega = 180^\circ$ ). The first letter refers to the torsional relationship between O6 and O5, and the second letter refers to the relationship between O6 and C4. All three conformations exist in solution as different populations depending on the properties of the solutions such as type of solvent, temperature or other molecules present.<sup>12–14</sup>

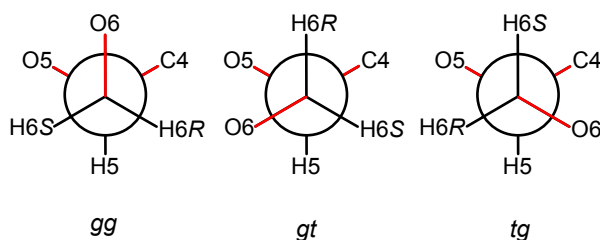


**Figure 2.3:** The three staggered conformations of the hydroxymethyl group on cellulose with the torsion relationships marked in red.

In nature, cellulose is found with two types of crystalline structures, namely, cellulose I $_{\alpha}$  and cellulose I $_{\beta}$ , which are found as a mixture of both structures in most plants.<sup>15</sup> The difference between the two forms is the size of the unit cell, i.e. how the chains hydrogen bond and prefer to associate with each other. However, synonymous for both cellulose I allomorphs is that the chains are arranged parallel to each other and that the hydroxymethyl group is found to be in the *tg* conformation.

Upon both thermal and chemical treatments, cellulose can adopt other crystalline structures. The most common ones are called cellulose II, III, and IV.<sup>16</sup> Cellulose I treated with alkali or dissolved and regenerated rearranges its crystalline structure to form cellulose II, and the hydroxymethyl group is then found in the *gt* conformation. The *gg* conformation is often represented in less ordered, i.e. amorphous, regions.<sup>17</sup> The cellulose II structure is thermodynamically more stable<sup>18</sup> and is characterised by the chains being arranged anti-parallel to each other. The change from a parallel into an anti-parallel arrangement is an interesting phenomenon still being discussed.<sup>19</sup> Cellulose III and IV are obtained through treatment at varying temperatures in liquid ammonia or other amines and glycerol, respectively.



## 2.2 Cellulose solubility

Dissolution of cellulose is an important process for many applications but is, however, challenging and, once again, brings the complex structure of cellulose to the fore. As mentioned in Section 2.1, a cellulose fibre is built up of several cell wall layers. Each cell wall layer has a certain composition and organisation that contributes to the properties of the wood. To obtain complete dissolution of a cellulose fibre, the solvent needs not only to be able to penetrate into the different cell walls but also to break all attractive forces between the cellulose chains. These forces involve both intra- and intermolecular hydrogen bonds and the interaction that leads to sheet stacking. Common solvents, such as water or dimethyl sulfoxide (DMSO), can only overcome the first stage, i.e. penetrate into the different cell walls, which in turn, causes swelling of the fibre. The second stage is more perplex, which is why the search for suitable cellulose solvents has become a relatively large scientific research area.<sup>16,20–29</sup>

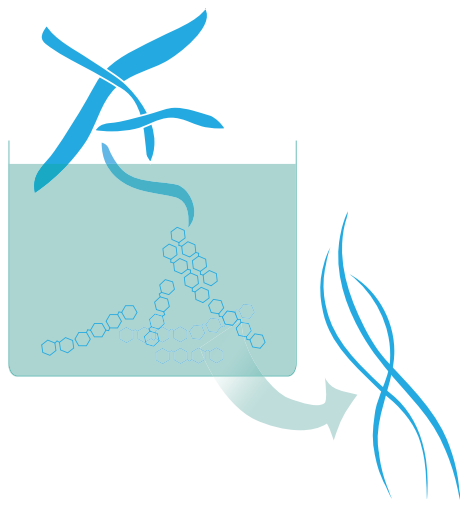


**Figure 2.4:** Schematic representation of the dissolution and reshaping process of cellulosic wood fibres. Adapted with permission from J. Bengtsson.

Although pulping processes can be used to purify wood fibres up to a cellulose content of more than 92%, so-called dissolving pulp grade, the native morphology of the fibres is not suitable for yarn spinning. Unlike cotton, which has long and thin fibres, wood fibres are short and thick, which gives them an as-

pect ratio (length to width ratio) that is too low for conversion directly into textile fibres. To overcome this obstacle, the native structure must be dissolved to obtain dissociated cellulose chains in a solution called a spin dope. Through spinning of the spin dope into an anti-solvent, the cellulose can be re-shaped into thinner and longer fibres (Figure 2.4).

There are, however, a number of solvents capable of a simultaneous breakage of all inherent forces in a cellulose fibre structure. A clear distinction is made between derivatising and non-derivatising solvents. A non-derivatising solvent is able of overcoming cellulose-cellulose interactions, whereas derivatising solvents accomplish derivatisation of the cellulose prior to dissolution. From a manufacturing perspective, direct solvents are preferred because they require one less processing step.

#### Derivatising solvents

A derivatising solvent performs a substitution reaction on the cellulose hydroxyl groups to promote solubility in a certain solvent. One of the oldest systems based on this is the viscose process, which still today, is the major method used for the production of textile fibres from wood. Alkali-treated cellulose is reacted with carbon disulfide to give the non-stable ester cellulose xanthate, which is soluble in dilute NaOH(aq) (Figure 2.5). A degree of substitution (DS) as low as 0.5 is enough to achieve efficient dissolution in dilute NaOH(aq). During the regeneration step, the viscose solution is spun into an acid solution, which hydrolyses the xanthate esters while the pure cellulose is regenerated into fibres. The substitution agent carbon disulfide is hazardous, which is why many old viscose mills are considered non-sustainable, but the implementation of closed-loop systems leads to great improvement in the environmental impact of the process.<sup>30</sup>

However, the low mechanical properties of the viscose fibres, especially during wet conditions, challenge the effort to find alternative processes to produce cellulose fibres with higher quality properties. An example of this is the cellulose carbamate process which uses urea instead in the substitution reaction on the cellulose fibres to obtain solubility in dilute NaOH(aq) (Figure 2.5). Unlike cellulose xanthate, cellulose carbamate is a stable ester, which means that the ester remains intact upon regeneration and can be removed in a subsequent processing step if wanted. The cellulose carbamate process is not yet commercially available but has recently reached pilot-scale production.<sup>31</sup>

The process uses fewer chemicals, and the fibres attain qualities equal to modified viscose fibres with improved wet strength.

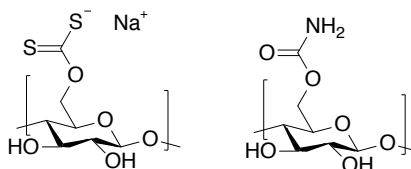


**Figure 2.5:** *The molecular structure of cellulose xanthate (left) and cellulose carbamate (right).*

Other derivatising solvents are formed by, for example, a reaction between the cellulose and formic acid to form cellulose formate, which is soluble in DMSO; dimethylformamide (DMF) and pyridine. Another example is the reaction between cellulose and trifluoroacetic acid or paraformaldehyde, which forms cellulose trifluoroacetate and methylol cellulose, respectively, and are both solubilised in DMSO during the derivatisation.<sup>32</sup> More recently, it was also found that cellulose dispersed in DMSO together with a so-called superbases, such as 1,8-Diazabicyclo[5.4.0]undec-7-ene (DBU), can be solubilised by the addition of CO<sub>2</sub> under pressure. The superbases is suggested to deprotonate the hydroxyl groups on cellulose, which initiates a nucleophilic attack on the CO<sub>2</sub> and the formation of a cellulose carbonate with the protonated superbases as a counterion.<sup>33</sup>

#### Non-derivatising solvents

A non-derivatising solvent possesses properties that can disrupt both a hydrogen bonding network and the stacking association that occur between the cellulose chains. In addition to this, the solvent must possess the driving force to penetrate the fibre structure. The dissolution process for a non-derivatising solvent has been identified to occur in different steps, depending on the quality of the solvent.<sup>34</sup> A high quality solvent, such as N-methylmorpholine N-oxide (NMMO), dissolves the cellulose fast *via* disintegration into rod-like fragments. A low quality solvent, such as cold NaOH(aq), dissolves the cellulose through initial swelling, followed by ballooning and then dissolution.

Although there are a number of direct solvent systems suitable for cellulose dissolution, only one is currently employed in a commercialised process, namely the lyocell process, which utilises NMMO as a direct solvent for cellulose. The dissolving mechanism of NMMO is reported to be the formation of one or two hydrogen bonds between the cellulose hydroxyl groups and the NO group in NMMO, which gives a stable complex due to the strong dipole moment of the NO group. The lyocell fibre is characterised by its high mechanical strength due to the superior orientation of the cellulose chain during spinning and subsequent drawing of the produced textile fibres. However, one drawback of the lyocell process is the thermal instability of the solvent, which can lead to an explosion but is nowadays controlled by the addition of stabilising agents in the spin dope. Further, the solvent must be recycled up to 99%, in order to maintain process sustainability, both environmentally and economically.

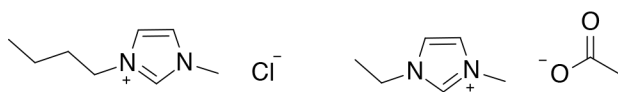


**Figure 2.6:** The molecular structure of 1-butyl-3-methylimidazolium chloride (BMIMCl) and 1-ethyl-3-methylimidazolium acetate (EMIMAc).

An alternative lyocell fibre could also be produced from so-called ionic liquids (IL), which, as indicated by their names, are liquid organic salts that possess intriguing properties. The first IL for the dissolution of cellulose was patented for liquefied quaternary ammonium salt as early as 1934.<sup>35</sup> In 2002, Swatloski et al. suggested that ILs synthesised from imidazolium, such as 1-butyl-3-methylimidazolium chloride (BMIMCl), would be promising for industrial applications that require cellulose dissolution.<sup>36</sup> By alternating the chemical structure of the cation or the anion, or both, there is no limit for the number of ILs that can be synthesised. Interestingly, all ILs are not solvents for cellulose which, again, describes the complexity of cellulose dissolution. Two of the most common ILs employed in cellulose research, both for developing applications and cellulose derivatives, are the aforementioned BMIMCl and 1-ethyl-3-methylimidazolium acetate (EMIMAc) (Figure 2.6). Like NMMO, ILs are reported capable of breaking the hydrogen bonds between the cellulose chains, thus causing cellulose to dissolve. In addition, it has been argued that the interaction between the cellulose and the anion plays the most important role in the

dissolution process but it has also been shown that the cation must fulfil certain structural requirements in order for the cellulose to dissolve in the IL.<sup>37</sup> However, the use of ILs on an industrial scale for textile fibre production is, at present, limited by the recyclability of the solvents, which is a demand from environmental and economical perspectives.

A non-derivatising solvent is attractive when looking at the reduced amount of processing steps it entails, but the need for specially developed solvents is an obstacle both to the production and regeneration of solvent. A solvent already familiar to an industry closely related to the production of textile fibres, such as the pulp and paper industry, is therefore an interesting option. This is also the reason why the water-based cold NaOH(aq) system once again has gained increased attention from both researchers and industry.



# 3

## The cold NaOH(aq) solvent system

*From an environmental point of view, an aqueous-based system for the dissolution of cellulose is of great interest. This is especially true for the NaOH(aq) system, since the chemical is used in several other process steps during pulp and paper production. For this reason, there is a well-developed infrastructure for handling of waste residues. The NaOH(aq) system is a promising solvent for cellulose, but it also possesses certain peculiarities, such as a narrow dissolution window and unstable solutions. New light has, therefore, been shed on the system over the last years to develop further insight on the dissolution mechanism and the interactions taking place between the solvent and the cellulose. This chapter describes the properties of the NaOH(aq) solvent and how its cellulose dissolution capacity can be modified with the addition of certain additives. In addition to the characteristics of the solvent, challenges to the investigation of molecular interactions that occur in the system are presented and briefly discussed in the chapter.*

### 3.1 Fundamentals of the NaOH(aq) cellulose dissolution system

The affinity between NaOH(aq) and cellulose has been known since the middle of the 19<sup>th</sup> century when John Mercer patented the mercerisation process to improve the properties of cotton fabric.<sup>38</sup> The invention describes the use of concentrated NaOH(aq) through the immersion of cotton fabric into the solution to improve lustre and dye uptake as well as mechanical properties and dimension stability. Later during the 19<sup>th</sup> century, the viscose process was developed where NaOH(aq) was used as an activating step towards reaction with a substituting agent.<sup>39</sup> The affinity between NaOH(aq) and cellulose is characterised by, first, the formation of different types of Na-cellulose intermediates, depending on the concentration of NaOH and the temperature of the solution and, second, the conversion from the cellulose I to cellulose II in crystalline structure. This process is not due to the dissolution of the cellulose fibre but to a change in morphology and crystalline structure that occurs in a highly swollen state during the formation of the different Na-cellulose complexes.<sup>4</sup>

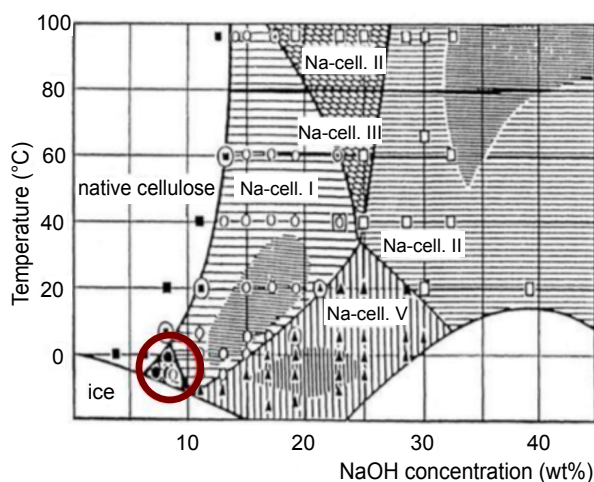


**Figure 3.1:** The NaOH(aq)/cellulose phase diagram adapted from Sobue et al. (1939)

The discovery of NaOH(aq) as a solvent for cellulose was patented as early as 1924 by Lilienfeld<sup>40</sup> and was later studied more in detail by Davidson,<sup>41</sup> who used partly hydrolysed cellulose to ease the dissolution process and found that a decrease in temperature improves dissolution in NaOH(aq). In 1939, Sobue et al. developed the ternary phase diagram for ramie cellulose, NaOH and water that



describes the regions for different Na-cellulose complexes as a function of NaOH concentration and temperature (Figure 3.1).<sup>42</sup> The region marked between -5 to +1°C and 7 to 10 wt% NaOH is referred to as the Q-state (*Quellung*, which means swelling in German) and is characterised by the phenomenon of cellulose dissolution occurring within this narrow window.

### Structure of cellulose/NaOH(aq) solutions

The phenomenon of NaOH(aq) working as cellulose solvent only at a certain concentration range and low temperature has been a puzzling research question over a long period of time, and great effort has been invested in identifying the structure of the solvent at different conditions and in the presence of cellulose. It is evident that the structure of the solvent, including both hydrated NaOH structures and the hydrogen bonding of water itself, are highly influenced by both the concentration of NaOH and the temperature of the solution. NaOH dissolves in water, giving two ions surrounded by water, i.e. hydrated ions. At a NaOH concentration below 20 wt%, water forms a primary and a secondary hydration shell around the ions. In the primary shell, the water is strongly bonded, which means that the ion and water move together. In the secondary shell, the water is less bonded, which suggests that these water molecules move freely around within this shell. At 10 wt% NaOH(aq) and +4°C, the primary and secondary shell is reported to consist of 8 and 23 water molecules, respectively.<sup>43</sup>

The narrow dissolution conditions for cellulose in NaOH(aq) must clearly be correlated to the structure of the ions as well as the bounded and freely moving water in the solvent. This has also been the explanation for the swelling behaviour of cotton caused by various aqueous alkali. The maximum swelling of cotton at a specific concentration has been found to be in the order  $\text{Li} > \text{Na} > \text{K} > \text{Rb} > \text{Cs}$ <sup>44</sup> and explained with the argument that the larger the ion the more difficult it is to penetrate into a cellulose fibre. Important to remember, though, is that this swelling behaviour occurs in diluted solutions where the ions are assumed to be maximum hydrated. Interestingly, although all aforementioned alkalis can swell cellulose, not all can dissolve it. The dissolution capacities decline according to their swelling capacity, once again suggested to be dependent on their type of hydration shell.<sup>45</sup>  $\text{Li}^+$  and  $\text{Na}^+$  can form two hydration shells, while  $\text{K}^+$  only forms one hydration shell with less strongly bonded water and, therefore, loses its dissolution capacity for cellulose. Thorough in-

vestigations by Roy et al.<sup>46</sup> and Egal et al.,<sup>47</sup> found that NaOH in water forms an eutectic structure, and in the presence of cellulose, the amount of this eutectic structure decreases. From this finding, the number of NaOH associated to the cellulose is calculated, which results in 4 moles NaOH per mole AGU. Considering the narrow dissolution window, the maximum dissolution capacity of an 8 wt% NaOH(aq) solution would then corresponds to 8 wt% cellulose.

### Stabilising interactions in a cellulose/NaOH(aq) solution

At specific conditions, NaOH(aq) is reported to break the hydrogen bonding network, and more specifically, the intermolecular  $O_3-H \cdots H_5'$  and  $O_2-H \cdots H_6'$  hydrogen bonds leading to dissolution.<sup>48</sup> Recently, the role of NaOH(aq) also acting as a deprotonating agent<sup>49</sup> was revisited and, again, it was suggested to be one of the driving forces for dissolution.<sup>50</sup> Deprotonation of the hydroxyl groups not only leads to breakage of the hydrogen bonding network but also to the formation of a polyelectrolyte and the introduction of repulsive forces between the cellulose chains. A close association between the cellulose chain and  $Na^+$  acting as a counterion for the deprotonated hydroxyl group has, though, not been possible to prove yet. The argument for hydrogen bonding breakage being the only force needed to achieve the dissolution of cellulose has, in recent years, been debated since the water-water, water-carbohydrate, and carbohydrate-carbohydrate hydrogen bonds are of the same bond strength, namely 5 kcal/mol.<sup>10</sup> There are evidently other forces that provide stability to the cohesive structure of the cellulose chains, which is why hydrophobic interactions have been suggested as an additional force to overcome when aiming for dissolution. The fact that additives, such as urea, which are known to break hydrophobic interactions and improve the dissolution of cellulose in NaOH(aq), supports this hypothesis.

The narrow process window of NaOH(aq) is a challenging factor for the industrial implementation of the system. Cellulose dissolved in NaOH(aq) must be kept between the temperatures of -10 and +10°C to remain in solution. As soon as the solution approaches the limits of this temperature interval, the cellulose chains start to associate to each other and precipitate as regenerated cellulose II. This temperature dependency clearly demonstrates that the chemical environment for the cellulose chains is optimal between -10 and +10°C, and must be maintained for the chains to remain in solution. If this dependency is solely at-

tributed to the properties of the solvent, or if the temperature also could have an effect on the conformation of the cellulose chains, which makes them more prone to dissolve in NaOH(aq), is still not fully understood. However, cellulose/NaOH(aq) solutions not only gel due to temperature changes, but exhibit another, more peculiar, feature of spontaneous gelation after dissolution, although the dissolution conditions remain, i.e. the same NaOH concentration and low temperature. Several theories for this behaviour have been framed. They point to the conversion from cellulose I to cellulose II during dissolution and a subsequent regeneration, and the fact that the cellulose II is less soluble in NaOH(aq) than cellulose I<sup>51</sup> or that external factors, such as the CO<sub>2</sub> in the surrounding air, could disrupt the quality of the solvent or interact with the dissolved cellulose and, thus, disturb the system.<sup>52</sup>

### 3.2 Impact of additives on dissolution in NaOH(aq)

In efforts to improve and optimise the dissolution of cellulose in NaOH(aq) several studies have evaluated different additives, both with the aim of increasing the dissolution rate and improving the stability of the solutions to ease handling of them prior to a regeneration step. The choice of additive can be determined based on the specific interaction desired to disrupt. In the beginning of the 1990's, Laszkiewicz et al. discovered that urea aids the dissolution of cellulose in NaOH(aq)<sup>53</sup> and that the dissolution rate of bacterial cellulose could be improved from 17% to 48.6% by the addition of 1 wt% urea.<sup>54</sup> As previously mentioned, urea is known to act as a denaturation agent for proteins by breaking the hydrophobic interactions that keep the crystal structure together.<sup>55</sup> It is, therefore, not surprising that urea has an effect on the dissolution of cellulose since it also belongs to the category of amphiphilic polymers. Moreover, urea has earlier been used in a way similar to NaOH(aq) to improve the qualities of cotton textile fabrics.<sup>56</sup> However, urea alone cannot dissolve cellulose but must be used in combination with another solvent in order to achieve dissolution. The true mechanism of urea in NaOH(aq) has not been fully proven yet, but its role in the dissolution process of cellulose has been studied by many research groups.<sup>4</sup> In summary, two theories have been proposed, namely, that urea impacts the quality of the solvent,<sup>57–59</sup> or that urea interacts with the cellulose through some type of binding.<sup>58,60–63</sup> A similar additive, thiourea, has also been found to promote dissolution in NaOH(aq) (Figure 3.2).<sup>64</sup>

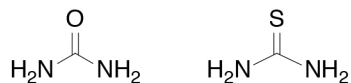


**Figure 3.2:** *The molecular structure of urea (left) and thiourea (right).*

Another category of dissolution- and stability-improving additives is metal oxides. Studies by Davidson show that metal oxides, such as zinc oxide, beryllium and aluminium oxides either improve or deteriorate dissolution of cellulose in aqueous alkali.<sup>65</sup> Interestingly, the hypothesis of using metal oxides for modifying the interaction between cellulose and NaOH(aq) was formulated based on the observation made by John Mercer that the swelling action of cotton caused by NaOH(aq) increased in the presences of zinc oxide. In NaOH(aq), zinc oxide (ZnO) converts to  $\text{Na}_2\text{Zn}(\text{OH})_4$ , (also known as sodium zincate) and has been reported to form stronger hydrogen bonds to cellulose than hydrates of NaOH.<sup>66</sup> ZnO has also been suggested as a binder for water, thereby decreasing the amount of free water surrounding the cellulose chains that otherwise promotes chain aggregation.

An unintentional additive in NaOH(aq) originates from the surrounding air as  $\text{CO}_2$  dissolves readily in NaOH(aq). When  $\text{CO}_2(\text{g})$  dissolves in NaOH(aq), it forms  $\text{CO}_2(\text{aq})$ , which instantly reacts with the  $\text{OH}^-$  to give  $\text{HCO}_3^-(\text{aq})$ . If the pH of the solution is above 10, the  $\text{HCO}_3^-(\text{aq})$  proceeds in a reaction with another  $\text{OH}^-$  and form  $\text{CO}_3^{2-}(\text{aq})$ . If the NaOH(aq) is let to stand in contact with the surrounding air, the pH of the solution will decrease, i.e. the  $\text{OH}^-$  will be consumed, which has a negative effect on the quality of the solvent. Interestingly, in 1927, Faurholt demonstrated that the presence of an alcohol, namely methanol, in NaOH(aq) increased the uptake of  $\text{CO}_2$  in NaOH(aq).<sup>67</sup> The mechanism was described as a deprotonation of the alcohol by the  $\text{OH}^-$  ions, which leads to a nucleophilic attack by the alkoxide on the  $\text{CO}_2(\text{aq})$  and results in the formation of an organic carbonate (Figure 3.3).

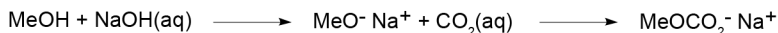


**Figure 3.3:** *The reaction mechanism between methanol (MeOH) dissolved in NaOH(aq) and  $\text{CO}_2(\text{aq})$ .*

In a more recent study on glycerol in NaOH(aq) it was found that the reaction between a glyceroxide, i.e. a deprotonated glycerol, and  $\text{CO}_2(\text{aq})$  is 6-7 times faster than the reaction between  $\text{OH}^-$  and  $\text{CO}_2(\text{aq})$ .<sup>68</sup> The former reaction is thereby favoured, even though the two reactions will occur in parallel in the solution. The actual impact of this reaction on cellulose dissolution in NaOH(aq) has not yet been thoroughly evaluated.

### 3.3 Analytical challenges of the cellulose/NaOH(aq) system

Analysis of the molecular interactions that occur in a cellulose/NaOH(aq) solution, with and without additives, demands analytical techniques that measure and report on the molecular level. This is, however, challenging in the NaOH(aq) for several reasons. Characterisation techniques that provide information on the size of the cellulose chains or the occurrence of aggregates in a solution, such as light scattering, demand purification of the solutions, i.e. filtration of a cellulose/NaOH(aq) solution, to remove other scattering particles, which is troublesome due to high viscosity of cellulose solutions and associated with substantial loss of dissolved material. Spectroscopic methods, such as infrared spectroscopy, can be used on both liquid and solid materials, but the large amount of water in the NaOH(aq) will saturate the spectrum and hide interesting features that occur between the cellulose, the additive, and the solvent. Analysis of a solid material, e.g. regenerated cellulose, can be of interest when evaluating the effect of different dissolution conditions and the addition of varying additives but will, again, not show how the solutes relate to each other.

The interaction between the different solutes can be analysed non-destructively on a molecular level with the use of nuclear magnetic resonance (NMR) spectroscopy. However, this procedure is limited by the dissolution capacity of the solvent. In other words, NMR spectroscopy demands high sample concentration, and the fact that the regular dissolving pulp cannot dissolve completely in the NaOH(aq) solvent results in low resolution of the obtained spectra and becomes an obstacle to such a type of molecular investigations. In addition to this, investigation of the true action of the NaOH(aq) during the dissolution of cellulose is difficult due to the lack of an appropriate reference solvent. Comparison of the structure of a cellulose analogue in a reference solvent such as water with equal ionic strength as the NaOH(aq), but neutral pH, can provide useful information on the NaOH(aq) dissolution mechanism. Taken together,

with a model compound, such as cellulose with lower DP or a monomer compound representing the repeating unit of cellulose, high resolution would be maintained owing to increased dissolution capacity.

# 4

## Methodology for understanding the molecular dimension of the cellulose/NaOH(aq) system and its controversies

*The dissolution mechanism for cellulose in NaOH(aq) has not yet been fully defined, but several theories on the driving forces have been developed and described. In order to investigate these theories on a molecular level, a representative model system is needed. This chapter describes the methodology for how to investigate certain controversies over the dissolution of cellulose in NaOH(aq).*

## 4.1 Investigating and understanding controversies of the cellulose/NaOH(aq) system

The focus of the thesis is on investigating existing hypotheses, which to some extent are controversial to each other, on the dissolution of cellulose in NaOH(aq) by elucidating the molecular interactions that occur in a pure system of NaOH(aq) and dissolved cellulose, and upon the addition of certain additives. The research issues of interest are:

- How to monitor the course of swelling and dissolution of cellulose in different aqueous alkalis at varying temperatures without affecting the original state of the sample (i.e. through disruptive sample preparation)
- The occurrence of conformational changes in a cellulose molecule induced by temperature changes and the addition of urea in NaOH(aq)
- The association of urea on certain surfaces, e.g. hydrophobic surfaces, of cellulose dissolved in NaOH(aq)
- Molecular interactions in NaOH(aq) containing CO<sub>2</sub> and dissolved cellulose with and without the presence of urea

## 4.2 Analytical tools and experimental setups

### NMR spectroscopy

Nuclear Magnetic Resonance (NMR) spectroscopy is an invaluable tool for the characterisation of molecular structures and their interactions and can be used to study all atoms (hereafter referred to as nuclei) with a nuclear spin quantum number greater than zero. Some of the most common nuclei used are <sup>1</sup>H, <sup>13</sup>C and <sup>15</sup>N. The wealth of methods provides information on the chemical structure of a molecule where each nucleus within the molecule is seen as a peak in a spectrum. Each peak is reported in terms of its chemical shift, which describes the chemical surrounding for each nucleus. Integration of the peaks also provides the opportunity of making a quantitative evaluation in relation to a reference peak. In addition to the chemical shift values, NMR also provides the possibility



of extracting data on the relationship between the different nuclei in the molecule, termed as the  $J$  coupling. Both homo and heteronuclear  $J$  couplings can be obtained, e.g.  $^1\text{H}$ - $^1\text{H}$  or  $^1\text{H}$ - $^{13}\text{C}$ , and be used further to evaluate and describe the conformation of a molecule and how this conformation is affected by variations in a certain system. Both the chemical shifts and the  $J$  coupling values are sensitive to alterations in the chemical surrounding of the molecules induced by, for example, the type of solvent used, temperature, or the presences of and interaction with other solutes.

NMR spectroscopy can be used both qualitatively and quantitatively, but the latter requires careful consideration of the experimental settings. Certain parameters are important to consider in order to obtain a quantitative spectrum. Two of those parameters are  $T_1$  and  $T_2$  which correspond to the spin-lattice and the spin-spin relaxation times, respectively. The former describes how long it takes for a nucleus to relax back to its initial state after being subjected to a radio-frequency (rf) pulse, and the latter describes how fast the signal generated by a  $90^\circ$  pulse decays during the acquisition of the signal. Large molecules, such as cellulose, have low  $T_2$  values, which is a highly limiting factor in obtaining an NMR measurement with high resolution since a low  $T_2$  value results in a spectrum with broad peaks of low resolution and intensity.

The aforementioned insufficient dissolution capacity of cellulose fibres in  $\text{NaOH(aq)}$  will also lead to a solution containing both a dissolved and an undissolved fraction, which is an obstacle for quantitative measurements. This obstacle is commonly overcome by solving for some type of separation of the two fractions, such as filtration, but will unfortunately also lead to a disruption of the original structure of the solution. To avoid this, representative model compounds withholding good dissolution capacity in  $\text{NaOH(aq)}$  were instead chosen as the cellulose substrate for the measurements in this thesis. Cellulose with a DP of 260, namely microcrystalline cellulose (MCC), obtained upon hydrolytical treatment, was chosen as the polymeric cellulose analogue, and methyl D-glucopyranoside (MeO-Glcp) with the protective methoxy group positioned in two different conformations ( $\alpha$ -MeO-Glcp and  $\beta$ -MeO-Glcp) was chosen as the monomeric cellulose analogue (Figure 4.1). The protective methoxy group at position C1 not only prevents ring opening in the  $\text{NaOH(aq)}$  and, thus, maintains chemical structure of the model substrate, but also gives a different acidity to the hydroxyl groups due to the difference in conformations.<sup>69</sup> Although the use of model substrates can reveal relevant molecular information

on the dissolution mechanism for cellulose in NaOH(aq), it is important to keep in mind that several contributing factors have been removed, such as the macromolecular structure, which of course will influence the dissolution mechanism.

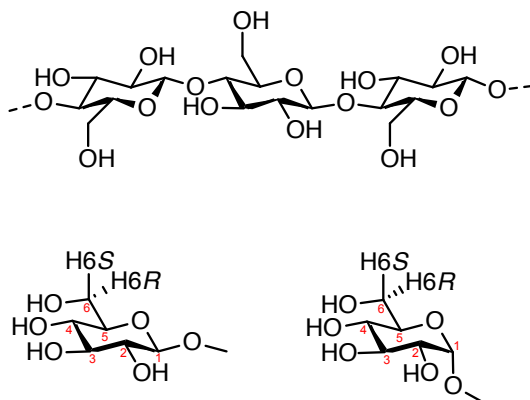


**Figure 4.1:** The molecular structure of the model compounds MCC (top),  $\beta$ -MeO-Glcp (bottom left) and  $\alpha$ -MeO-Glcp (bottom right).

For the NMR investigations, samples were prepared by either dissolving MCC or the  $\alpha$ -/ $\beta$ -MeO-Glcp in NaOH(aq) at  $-5^{\circ}\text{C}$  with or without the addition of an additive (the preparation is described in detail in the appended papers). Samples were then characterised using several NMR methods in combination with the complementary methods presented in the following section. Figure 4.2a) shows a schematic illustration of a typical  $^1\text{H}$  measurement where the flat line in the beginning represents a delay, typically in the order of a couple of seconds. A delay of  $5 \times T_1$  is needed to obtain a quantitative information. The vertical box represents the rf pulse that is applied to obtain a signal from the nucleus. This is followed by a wave, which represents the free induction decay (FID). The decay of the FID is of the same order of magnitude as the molecule's  $T_2$  value. The recorded FID is, thereafter, Fourier transformed into the spectrum.

$^1\text{H}$  and  $^{13}\text{C}$  measurement were performed as illustrated in Figure 4.2a) and b), where  $^1\text{H}$  decoupling was used during the acquisition of the  $^{13}\text{C}$  to eliminate the  $J$  couplings, which results in one peak for each carbon in the molecule. From these experiments, the chemical shift values for MCC and  $\alpha$ -/ $\beta$ -MeO-Glcp could be extracted and evaluated in terms of the molecular interactions that

occur in NaOH(aq) containing CO<sub>2</sub> and dissolved cellulose with and without urea (paper I-V). The same experiments, but without the <sup>1</sup>H decoupling during the acquisition of the <sup>13</sup>C, were used to obtain the <sup>1</sup>H-<sup>1</sup>H and <sup>1</sup>H-<sup>13</sup>C *J* coupling values to investigate the occurrence of conformational changes in β-MeO-Glcp induced by temperature and the addition of urea in NaOH(aq) (Paper V).

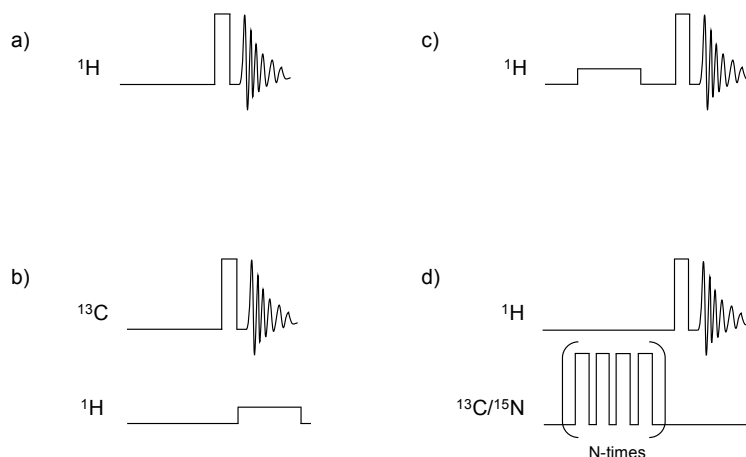


**Figure 4.2:** Schematic representations of the experimental setups for a) <sup>1</sup>H, b) <sup>13</sup>C, c) magnetisation transfer (MT) and d) heteronuclear Overhauser effect (HOE) NMR measurement.

An additional feature of NMR spectroscopy is the presence of the so-called nuclear Overhauser effect (NOE), which is the ability of a nucleus to transfer magnetisation through space when nuclei are close enough to each other. By measuring the NOE, it is possible to elucidate whether or not two molecules are close to each other and, consequently, interact with each other as the signal intensity increases or decreases for the detected nucleus due to the transferred magnetisation. Figure 4.2c) illustrates an experiment referred to as magnetisation transfer (MT) where a nucleus that resonates at a certain frequency, denoted frequency offset, is irradiated in the beginning to transfer its magnetisation to other molecules close in space after which a <sup>1</sup>H spectrum is recorded (Figure 4.2a)). This method was used to monitor the course of swelling and dissolution of cellulose in different aqueous alkalis at varying temperatures without affecting the original state of the sample (i.e. through disruptive sample preparation). A schematic representation of the method is shown in Figure 4.3

where the water dynamics based on  $k_{\text{on}}$  (bound water) and  $k_{\text{off}}$  (free water) are evaluated to describe the degree of cellulose swelling (Paper VI).

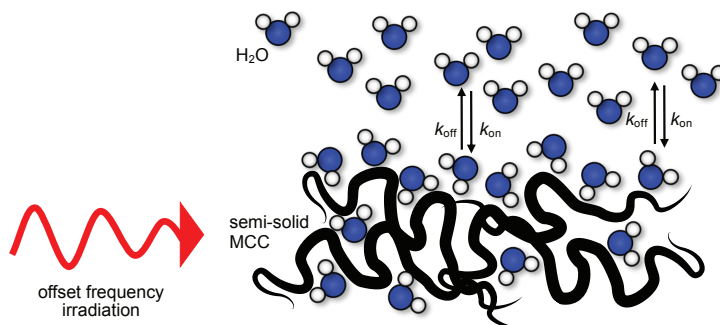


**Figure 4.3:** Schematic representation of a magnetisation transfer experiment where  $\text{H}_2\text{O}$  molecules exchange with "bound and immobile  $\text{H}_2\text{O}$ " on the  $k_{\text{on}}$  and  $k_{\text{off}}$  time scale monitored by the use of an offset frequency irradiation.

NOE also exists heteronuclearly and is then called heteronuclear Overhauser effect (HOE). The HOE was used to evaluate molecular interactions in  $\text{NaOH(aq)}$  containing  $\text{CO}_2$  and dissolved cellulose with and without the presence of urea. The HOE was also used to evaluate the association of urea on certain surfaces, e.g. hydrophobic surfaces, of cellulose dissolved in  $\text{NaOH(aq)}$  (Figure 4.2d). The evaluation was done through a comparison of a spectrum with irradiation of either  $^{13}\text{CO}_3^{2-}$  or urea- $^{15}\text{N}$  with a regular  $^1\text{H}$  spectrum without the irradiation. The low abundance of some nuclei requires labelled compounds to achieve sufficient transfer of the magnetisation from e.g.  $^{13}\text{CO}_3^{2-}$  or urea to the nuclei detected, in this case  $^1\text{H}$ . This was why  $^{13}\text{CO}_3^{2-}$  and urea- $^{15}\text{N}$  were used in the samples (Papers III-V).

Through the use of the same experimental setup on both the systems of interest and a reference system, a comparable analysis can be performed of how the different parameters affect the chemical features of the molecule at different conditions. A reference solvent for the  $\beta$ -MeO-Glcp and  $\alpha$ -MeO-Glcp,  $\text{D}_2\text{O}/\text{NaCl}$ , was used at the same concentration as the actual solvent  $\text{D}_2\text{O}/\text{NaOH}$ . The sample preparation is described in detail in the appended papers.

## Complementary methods

In addition to the NMR measurements, complementary methods were used to obtain more insight into the properties of the investigated system. Attenuated total reflectance Fourier transform infrared (ATR-FTIR) spectroscopy was used on precipitated MCC subjected to  $\text{CO}_2$  during dissolution. The precipitated MCC was then evaluate in terms of molecular alterations had by  $\text{CO}_2$  sorption in  $\text{NaOH(aq)}$  or  $\text{NaOH(aq)}$  with addition of urea. Static and dynamic light scattering were used to investigate the macromolecular structure of MCC dissolved in  $\text{NaOH(aq)}$ , both without additives and in the presence of  $\text{CO}_2$  or/and urea. The pH of all systems was measured prior to the NMR measurements to establish the difference in activity of the ions in the system and to clarify the need to keep this property in mind when comparing and evaluating different systems against each other.



# 5

## Driving forces for dissolution of cellulose in aqueous alkalis

*The course of swelling and dissolution of cellulose in aqueous alkali is key in order to gain a mechanistic understanding of the driving forces for cellulose dissolution in NaOH(aq). Nonetheless, characterisation of swelling and dissolution of cellulose without disrupting the original state of the sample is challenging. In this chapter, based on Paper VI, the use of an NMR method denoted MT is investigated and evaluated for monitoring the swelling and dissolution of MCC in three different aqueous alkalis.*

## 5.1 Cellulose dissolution capacity of different aqueous alkalis as a function of temperature

The intriguing observation that only a few aqueous alkalis possess the ability to dissolve cellulose disclose that the role of the cation is of importance. The role of the anion as an enabler of breaking hydrogen bonds cannot solely be decisive for efficient dissolution. pH measurements of the three different aqueous alkalis, namely, LiOH, NaOH, and KOH, usually studied for the dissolution of cellulose reveal that the discussed deprotonation of cellulose as the driving force for dissolution cannot be the sole mechanism. This is because KOH(aq) was found to have the highest pH of the three solvents at the same concentration and temperature (Table 5.1). In other words, if deprotonation was the determining driving force for dissolution, KOH(aq) would possess the highest dissolution rate of all three solvents, which has been reported not to be the case.<sup>41</sup>

**Table 5.1:** *The pH of aqueous alkali solutions at 0.5 M and +10°C*

Sample	pH
LiOH	13.67
NaOH	13.96
KOH	> 14

By following the dissolution process in different aqueous alkalis, valuable information can be obtained on the dissolution mechanism and on the roles of the different ions. NMR spectroscopy provides the opportunity of quantitatively determining the dissolution capacity of the different solvents and elucidating on the relaxometry of both the solvent and the cellulose without interfering the original state of the sample, which is often the case in other characterisation techniques such as light scattering. NMR-analysis of the dispersion of MCC (0.4 M) in the three above mentioned aqueous alkalis (2.0 M) transferred to NMR tubes, which were pre-frozen and thawed at -10, -5, and +5°C while the NMR experiments were performed, was found to be a non-disruptive method to monitor the dissolution process.

A quantitative determination of the cellulose dissolution capacity in the different solvents was performed by integrating the  $^1\text{H}$  spectrum of MCC in all three solvents and temperatures to calculate the amount of dissolved MCC and eval-



uate it against the maximum amount added to the samples. An example of a  $^1\text{H}$  spectrum is shown in Figure 5.1a). This example corresponds to the MCC dissolved in  $\text{LiOH(aq)}$  at  $-5^\circ\text{C}$ . The  $\text{H}_2\text{O}$  peak was set to 0 ppm due to subsequent evaluation of this peak in the MT measurements presented in Section 5.3.

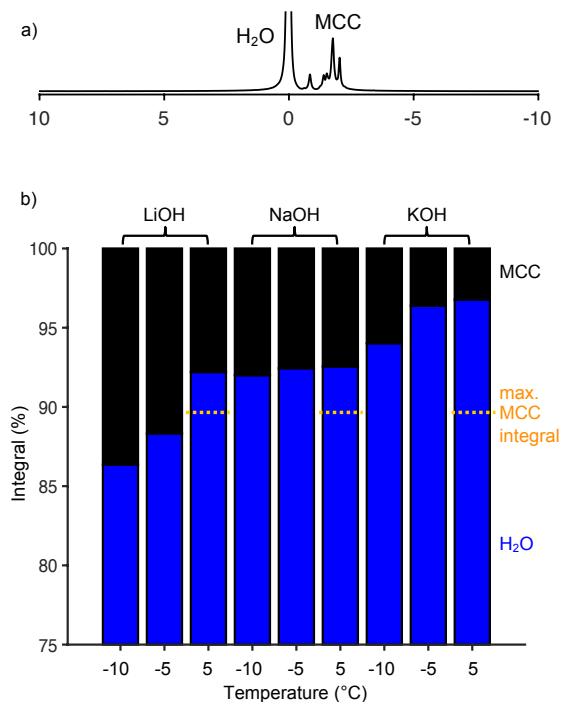


**Figure 5.1:** The measured amount of dissolved MCC in 2.0 M  $\text{LiOH(aq)}$ ,  $\text{NaOH(aq)}$  and  $\text{KOH(aq)}$  from the integration of the corresponding  $^1\text{H}$  spectra at various temperatures in relation to the amount of  $\text{H}_2\text{O}$  present in the solution. The maximum amount of MCC added to the solution is marked in orange.

Interestingly, as shown in Figure 5.1b), all three solvents were able to dissolve cellulose but to different extents. This is in agreement with earlier results reported by Davidson<sup>65</sup> but is not in agreement with those reported by Xiong et al.<sup>45</sup> and Cai et al.,<sup>70</sup> who have stated that  $\text{KOH(aq)}$  cannot dissolve cellulose fibres. The MCC, however, appears to be a different case as roughly 25% was found to be dissolved at  $+5^\circ\text{C}$  in  $\text{KOH(aq)}$ . In  $\text{LiOH(aq)}$  and  $\text{NaOH(aq)}$ , 70% of the added MCC was dissolved at  $+5^\circ\text{C}$ , which is in agreement with the observations made earlier by Alves et al..<sup>27</sup> Intriguingly, at the lower temperatures  $-10$  and  $-5^\circ$ ,

LiOH(aq) was found to dissolve more than the maximum amount of MCC added. Observable  $^1\text{H}$  signals arise from NMR-detectable (i.e. non-frozen) water and MCC, which is why this finding is suggested to be due to a lower amount of NMR-detectable  $\text{H}_2\text{O}$ , i.e. a lower amount of  $\text{H}_2\text{O}$  was non-frozen at  $-10$  and  $-5^\circ\text{C}$ . LiOH(aq) has, however, a lower freezing point than both NaOH(aq) and KOH(aq),<sup>71</sup> which indicates that the addition of MCC impacts the freezing behaviour of water. This is further strengthened by the detected amount of dissolved MCC found to decrease with temperature and at  $+5^\circ\text{C}$ , thus, passing the maximum amount mark. The same phenomenon of a decreasing amount of dissolved MCC at increased temperature was also found in KOH(aq), which, however, was more likely due to a decrease in dissolution capacity of the solvent with increasing temperature since KOH(aq) exhibits the lowest freezing-point depression of the three solvents. Interestingly, this was not the case for NaOH(aq) as the amount of dissolved MCC measured only changed slightly with increasing temperature, which could be an indication that the amount of dissolved MCC and non-frozen  $\text{H}_2\text{O}$  changed simultaneously and that NaOH(aq) is a more effective solvent for cellulose than KOH(aq) within this temperature range.

## 5.2 Relaxation rates of $\text{H}_2\text{O}$ and MCC in different aqueous alkalis at increasing temperature

The difference found in the dissolution capacity of the three solvents could be manifested further when the mean  $T_1$  value for the non-frozen  $\text{H}_2\text{O}$  and MCC is evaluated at the different temperatures. The  $T_1$  value is converted into the mean spin-relaxation rates  $R_1$  through the relationship  $1/T_1$ , and plotted in an Arrhenius plot against the inverse temperature to investigate the effect of the temperature changes (Figure 5.2). The  $R_1$  for non-frozen  $\text{H}_2\text{O}$  was found to be a straight line for all three solvents, where LiOH(aq) had the steepest slope and KOH(aq) had the lowest. Upon the addition of MCC, the  $R_1$  for the non-frozen  $\text{H}_2\text{O}$  appeared to be unaffected. However, the  $R_1$  for MCC was found to exhibit a different relation against temperature as the temperature plateaued at  $-5^\circ\text{C}$  in all solvents. This is interesting since the optimal dissolution temperature of cellulose in aqueous alkali is reported to be around  $-5^\circ\text{C}$ . In addition to this, it was found that, in the presence of urea in the NaOH(aq), the plateau moved to a temperature below  $-15^\circ\text{C}$ , which suggests different prerequisites for this solvent.

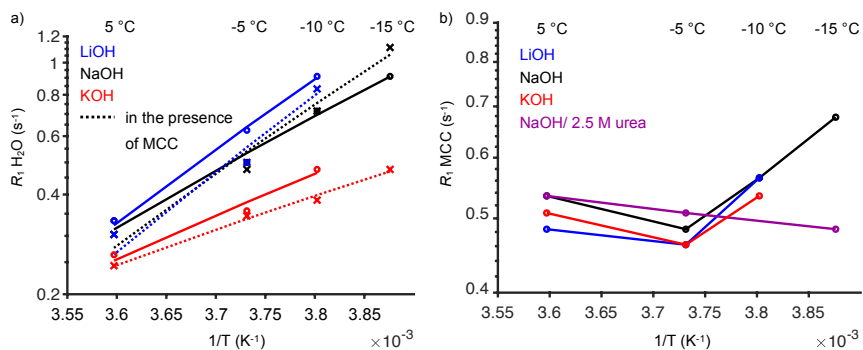


**Figure 5.2:** The mean spin-relaxation rates as a function of temperature in an Arrhenius plot for non-frozen  $\text{H}_2\text{O}$  a) and MCC b). In a), the straight lines represent the data points fitted to pseudo-Arrhenius behaviour, and in b), the lines are guides for the eye.

An interesting feature of the different solvents was also observed when the mean  $T_2$  value for the non-frozen  $\text{H}_2\text{O}$  in relation to temperature in an Arrhenius plot (Figure 5.3) was evaluated. In  $\text{LiOH(aq)}$ , the mean  $T_2$  of  $\text{H}_2\text{O}$  remained constant with temperature, while in  $\text{NaOH(aq)}$  and  $\text{KOH(aq)}$ , the mean  $T_2$  of  $\text{H}_2\text{O}$  increased with temperature.

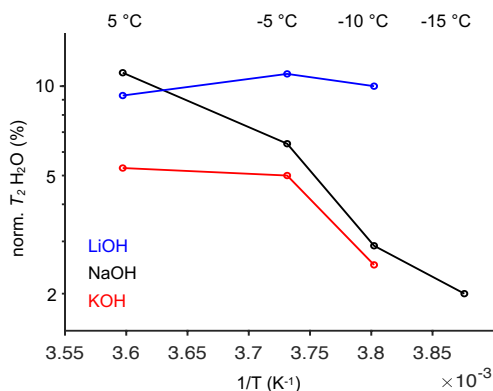


**Figure 5.3:** The mean  $T_2$  of  $\text{H}_2\text{O}$  in  $\text{LiOH(aq)}$  (blue),  $\text{NaOH(aq)}$  (black) and  $\text{KOH(aq)}$  (red) containing MCC at different temperatures normalised against the mean  $T_2$  of  $\text{H}_2\text{O}$  in the reference solvents.

The addition of MCC was found to influence the mean  $T_2$  of  $\text{H}_2\text{O}$  the most in  $\text{KOH(aq)}$ . The  $T_2$ s are most likely affected by exchange of water molecules

with the hydroxyl groups on the dissolved MCC and with the water that is associated with the semi-rigid MCC. This will be discussed in the evaluation of using magnetisation transfer for the purpose of monitoring cellulose swelling in the Section 5.3.

### 5.3 Magnetisation transfer as a tool for monitoring swelling of cellulose

Magnetisation transfer as an NMR method has been used in other research fields to measure the exchange rate of  $\text{H}_2\text{O}$  with mobile/exchangeable protons present in OH- or  $\text{NH}_2$ -groups that resonate close to the water peak in an  $^1\text{H}$  NMR spectrum. This is only visible when the exchange rate is slower than approximately 100 Hz. In addition to this, magnetisation transfer NMR is able to monitor protons associated to semi-rigid polymers or tissues, which are invisible with conventional  $^1\text{H}$  NMR due to their short  $T_2$ s.<sup>72</sup> As illustrated in Figure 4.3, bulk  $\text{H}_2\text{O}$  exchanges with "bound and immobile"  $\text{H}_2\text{O}$  on a semi-rigid cellulose, which remains associated for timescales shorter than the exchange rate  $k_{\text{off}}$ . The association results in an invisible signal that possibly covers a range between 10-150 ppm, which is too broad to be detected because of short  $T^2$ s and homonuclear couplings, which might be up to 70 kHz.

However, when this signal is irradiated at an offset frequency, the "bound and immobile" water molecules will transfer their magnetisation to the bulk water molecules if there is an exchange not faster than  $10^3$  Hz.<sup>73</sup> Hence, an MT spectrum, or a so-called *Z*-spectrum, displays the intensity of the water peak as a function of the irradiation frequency. If an exchange process between water molecules and the dissolved MCC, whose H1-H6 peaks in this representation resonate at negative ppm values while its hydroxyl groups appear at positive ppm values, would occur at a rate slower than  $10^3$  Hz, the *Z*-spectrum would show a dip at the position where the exchange happens. The exchange rate at this high pH in aqueous alkali is, however, expected to be much faster,<sup>74</sup> which explains why the *Z*-spectra shown in Figure 5.4 lack these features.

Interestingly, the *Z* spectra was instead able to display different shapes at the varying temperatures of the three solvents with MCC. The width is suggested to be attributed to the swollen state of semi-rigid MCC, which mainly depends on the  $1/T_2$  of the protons associated to the semi-solid fraction.<sup>75</sup>

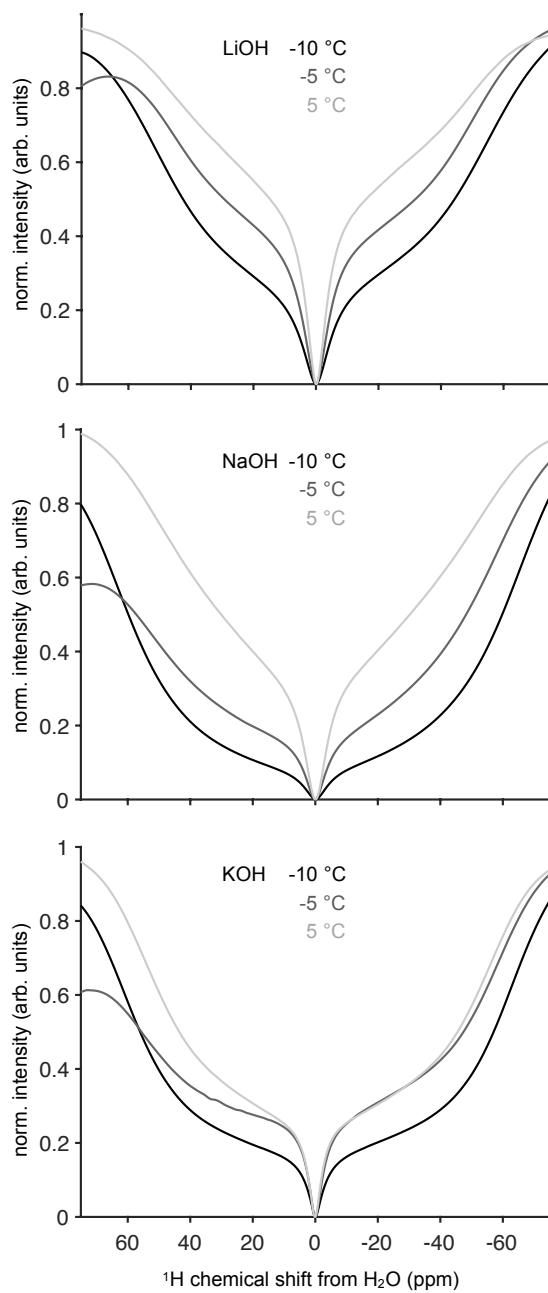


**Figure 5.4:** Magnetisation transfer spectra for  $\text{LiOH(aq)}$ ,  $\text{NaOH(aq)}$  and  $\text{KOH(aq)}$ , top to bottom. The chemical shift is normalised to the  $\text{H}_2\text{O}$  peak set to 0 ppm.

At -10°C, NaOH(aq) and KOH were found to have a similar broad width, and LiOH(aq) had a more narrow width, which suggests that the semi-solid MCC was more swollen for LiOH. In other words, the broadening of the curve for LiOH(aq) started first above 0.2 of the normalised intensity, which indicates that the fraction of semi-rigid MCC was lower than the fractions in KOH(aq) and NaOH(aq). Instead of the width changing with temperature, as for NaOH(aq) and KOH(aq), the fraction changed with temperature for LiOH(aq). At +5°C, all solvents revealed a broad feature, which is in line with the results from the  $^1\text{H}$ s integrals that showed a fraction of non-dissolved MCC, with the largest fraction found for KOH(aq). In NaOH(aq), both the normalised intensity and the width changed from -5 to +5°C, which could be because of a greater swelling within this temperature range. Plausibly, this result could be related to the reported decrease in the intrinsic viscosity of cellulose in NaOH(aq) with increasing temperature.<sup>76,77</sup>

The use of magnetisation transfer for monitoring the swelling of cellulose is, however, largely dependent on many parameters. Some of those parameters are the exchange rate of  $k_{\text{on}}$  and  $k_{\text{off}}$ , the  $T_1$  and  $T_2$  of water and the semi-rigid MCC fractions, the saturation duration and the  $B_1$  field of the saturation RF pulse. Upon optimisation, the method is, therefore, believed to have potential to contribute to valuable information on the cellulose/NaOH(aq) system. Information from a more optimised MT experiment can, in conjunction with recent reported modelling results, be useful to elucidate if the concentration of water is higher around the hydroxyl groups<sup>78</sup> or if there is a more tightly coordinated water structure close to the microfibrillar cellulose chains.<sup>79</sup>

In summary, the evaluation of quantitative  $^1\text{H}$  integrals of MCC dispersed in a solvent upon thawing at different temperatures in combination with relaxation evaluation and measurements of a  $Z$ -spectrum was found to have potential for elucidating the swelling and dissolution process of cellulose in aqueous alkali. The method, however, requires further optimisation in terms of influencing parameters, which should be done with respect to reported modelling results to confirm important properties of the system. Interestingly, the clear distinction in dissolution capacity between NaOH(aq) and KOH(aq) falls in line with the phenomenon of a so-called reversed Hofmeister series.<sup>80</sup> In a normal Hofmeister series, ions of a certain bare ionic radius are considered as hydrophilic or hydrophobic.  $\text{Li}^+$  and  $\text{Na}^+$  are considered hydrophilic and strongly hydrated, and  $\text{K}^+$  is considered as hydrophobic and weakly hydrated. This means that when a hydrophobic surface, such as a hydrophobic surface of the amphiphilic cellu-

lose, is introduced in the solvent, the more hydrophobic  $K^+$  ion will accumulate on the surface to minimize its free energy, while  $Li^+$  and  $Na^+$  remains associated with the solvent, which is energetically the most favourable state for a hydrophilic ion. However, in the case of a reversed Hofmeister series, the hydrophobic surface is considered to be deprotonated due to an increase in pH, e.g. the hydroxyl groups on cellulose become deprotonated. Deprotonation of the surface increases its hydrogen bonding with  $H_2O$ , which in turn leads to an expulsion of the  $K^+$  ion from the surface as  $H_2O$  and strongly hydrated ions, such as  $Li^+$  and  $Na^+$ , minimize their free energy when binding to the surface. In other words, deprotonation in combination with sufficient binding of water, both by the cellulose and the ions present, could be an explanation for the difference in the dissolution capacity of cold aqueous alkalis.





# 6

## Conformational changes promoting dissolution

*The peculiar behaviour of cellulose to only dissolve in NaOH(aq) at low temperature has been suggested to be the result of conformational changes in the cellulose induced by the low temperature.<sup>81</sup> Consequently, this promotes a conformation of the cellulose that is more prone to dissolve in polar solvent. Conformational changes have also been indicated as the driving force for the increase in the dissolution capacity of cellulose in NaOH(aq) upon the addition of urea, where the urea is suggested to accumulate on the hydrophobic surfaces of cellulose and, thus, promote dissolution. In this chapter, based on Paper V, the conformational changes of the cellulose model compound  $\beta$ -MeO-Glcp are evaluated as a function of temperature and the addition of urea to the NaOH(aq) solvent. The proposed association between cellulose and urea is also elucidated on a molecular level.*

## 6.1 Solvent effects on $J_{HH}$ coupling values

The fact that NaOH(aq) is a better solvent for cellulose than KOH(aq) points out a certain ability of the former solvent to provide a more beneficial chemical environment for the polymer to dissolve in. The amphiphilic nature of cellulose suggests that the NaOH(aq), as a solvent, has specific properties in which the cellulose is more willing to expose not only its polar sides but also the non-polar surfaces of the glucose ring. The exposure results in dissolution promoted by conformational changes and the disruption of stabilisation forces. The improved dissolution of cellulose in the presence of urea would then be assumed to be promoted by an even more beneficial conformational change where the urea is assumed to e.g. accumulate on the non-polar surface.

**Table 6.1:** Difference in  $^3J_{HH}$  couplings (Hz) of  $\beta$ -MeO-Glcp when dissolved in NaOH(aq) or NaOH(aq) with urea in comparison to NaCl(aq) or NaCl(aq) with urea, respectively, at +5°C. The significant changes are marked in red.

$^1\text{H}$ position	$\delta(\text{Hz})$ NaOH(aq)	$\delta(\text{Hz})$ NaOH(aq) with urea
H1	-0.2	-0.1
H2	-0.5	-0.5
H2	-0.3	0.2
H3	-0.4	-0.4
H3	-0.4	-0.4
H4	-0.4	-0.2
H4	-0.2	-0.2
H5	0.2	0.5
H5	<b>1.1</b>	<b>1.0</b>
H5	-0.6	-0.3
H6 <sub>R</sub>	<b>1.0</b>	<b>0.8</b>
<sup>a</sup> H6 <sub>R</sub>	-0.2	-0.3
H6 <sub>S</sub>	0.2	0.2
<sup>a</sup> H6 <sub>S</sub>	-0.2	-0.2

<sup>a</sup>  $^2J_{HH}$  couplings

To evaluate this on a molecular level with high resolution,  $^{2,3}J_{HH}$  coupling values, which reflect the conformational configuration, were measured using  $^1\text{H}$ - $^1\text{H}$  J-resolved NMR spectroscopy for the cellulose model compound  $\beta$ -MeO-Glcp dissolved in NaOH(aq) (2.0 M) or NaOH(aq) (2.0 M) with urea (2.5 M) and

evaluated in comparison to NaCl(aq) or NaCl(aq) with urea as the reference solvent.

The  $J_{HH}$  couplings obtained from the measurements correspond to the distance between both protons sitting on the same carbon (two bonds away) and neighbouring protons (three bonds away), denoted as  $^2J_{HH}$  and  $^3J_{HH}$  couplings, respectively. These couplings are on the order of 2-12 Hz, which is challenging to measure with an accuracy of more than 1 Hz. Evaluation of the coupling values showed that, for most of the protons, only minor differences occurred in the comparison between NaOH(aq) and NaCl(aq) and in the presence of urea (Table 6.1). However, the neighbouring protons H5 and H6R showed a more significant change of about 1 Hz when going from NaCl(aq) to NaOH(aq). The same was true in the presence of urea, which suggests the change to occur owing to the change in pH.

To obtain conformational information from this change, different types of equations have been developed to describe the change in the torsional angle from the coupling values as shown in Figure 2.3. Equation 6.1 describes the torsion angles for H5,H6R, developed by Stenutz et al.<sup>13</sup> Figure 6.1 shows that the torsion angle decreases slightly when going from NaCl(aq) to NaOH(aq), which corresponds to an increase in the population of the *gt* rotamer since all rotamers exist to different extent in the solution. The *gt* rotamer is the most stable rotamer, owing to the hydrogen bonding between the hydroxyl group and the ring oxygen, and the fact that different hydroxymethyl rotamers possess different solvation shells, depending on the surrounding solvent.<sup>12</sup>

$$^3J_{H5,H6R} = 5.08 + 0.47\cos(w) + 0.90\sin(w) - 0.12\cos(2w) + 4.86\sin(2w) \quad (6.1)$$

In addition to this, the change in solvent was found to decrease the  $^1H$  chemical shifts because of the increase in pH, which leads to partial deprotonation of the hydroxyl groups.<sup>50</sup> However, as the change in temperature did neither impacted the chemical shift values nor the  $J_{HH}$  couplings, which is in accordance with the result from Bergenstr hle-Wohlert et al.,<sup>82</sup> the conformational change in the hydroxymethyl group cannot be the solely driving force for the dissolution of cellulose in NaOH(aq).

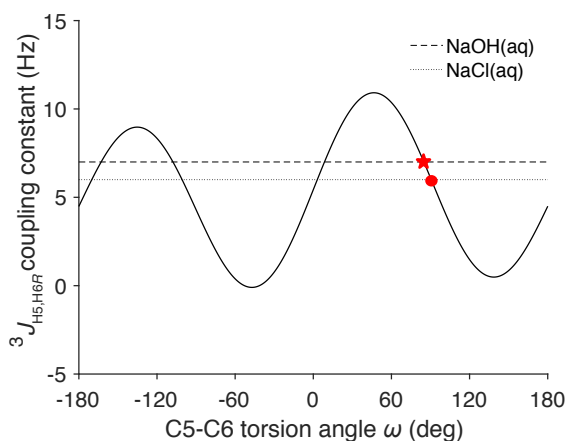


**Figure 6.1:** The experimental  $^3J_{H5,H6R}$  coupling constants in NaCl(aq) or NaOH(aq) plotted against the torsion angles calculated from 6.1. The torsion angles in NaCl(aq) and NaOH(aq) are marked with a circle and a star, respectively.

## 6.2 Temperature effects on chemical shifts and $^1J_{CH}$ coupling values

Similar to the measurement of the  $J_{HH}$  couplings, a  $^{13}C$  spectrum can be recorded without  $^1H$  decoupling during acquisition to obtain both the  $^{13}C$  chemical shifts and the  $^1J_{CH}$  coupling values. These couplings are on the order of 130-150 Hz and describe the distance of between the carbon and its attached proton. In contrast to the results from the  $^1H$  spectra, both the  $^{13}C$  chemical shifts and the  $^1J_{CH}$  couplings appeared to be influenced by both variation in temperature and the addition of urea in the NaOH(aq) solvent.

The chemical shift values for the different carbons in  $\beta$ -MeO-Glcp were found to decrease by the increase in temperature from -10 to +5°C (Figure 6.2). Interestingly, the decrease was different for the different carbons where positions C1, C3, and C5 experienced the largest decrease in chemical shift. Upon the addition of urea, positions C3 and C5 were the most affected, which suggests that these positions are the most sensitive to changes in the chemical environment. The changes of chemical shifts induced by the temperature alteration and addition of urea were absent in the NaCl(aq) solvent, which suggests that the observed changes could be attributed to the properties of the

NaOH(aq) solvent in combination with partial deprotonation of the hydroxyl groups.

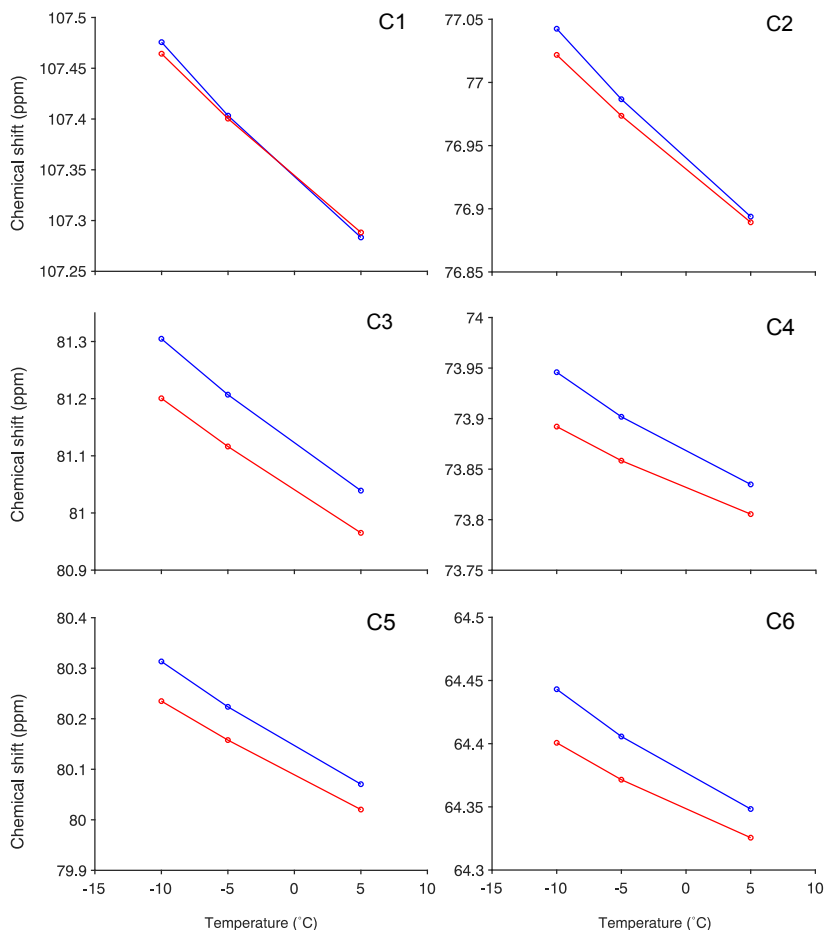


**Figure 6.2:** Chemical shift change for each carbon in  $\beta$ -MeO-Glcp dissolved in NaOH(aq) (blue) or NaOH(aq) with urea (red) in comparison to NaCl(aq) or NaCl(aq) with urea, respectively, and as a function of temperature. All measurements were recorded in  $D_2O$ .

Further, the  $^1J_{CH}$  couplings of the different carbons were also found to be affected differently as a function of temperature (Figure 6.3). A comparison of the  $^1J_{CH}$  couplings in NaOH(aq) with NaCl(aq) showed that all positions experienced a decrease in coupling value except for position C3, which showed an increase. The increase at position C3 was also found to be further promoted with

increased temperature. Interestingly, this phenomenon was found to be even more distinct with the addition of urea. The largest decrease in  $^1J_{CH}$  coupling was found for position C2. This is not surprising owing to the fact that this position is the most acidic one and, therefore, is the one most prone to deprotonation in NaOH(aq).

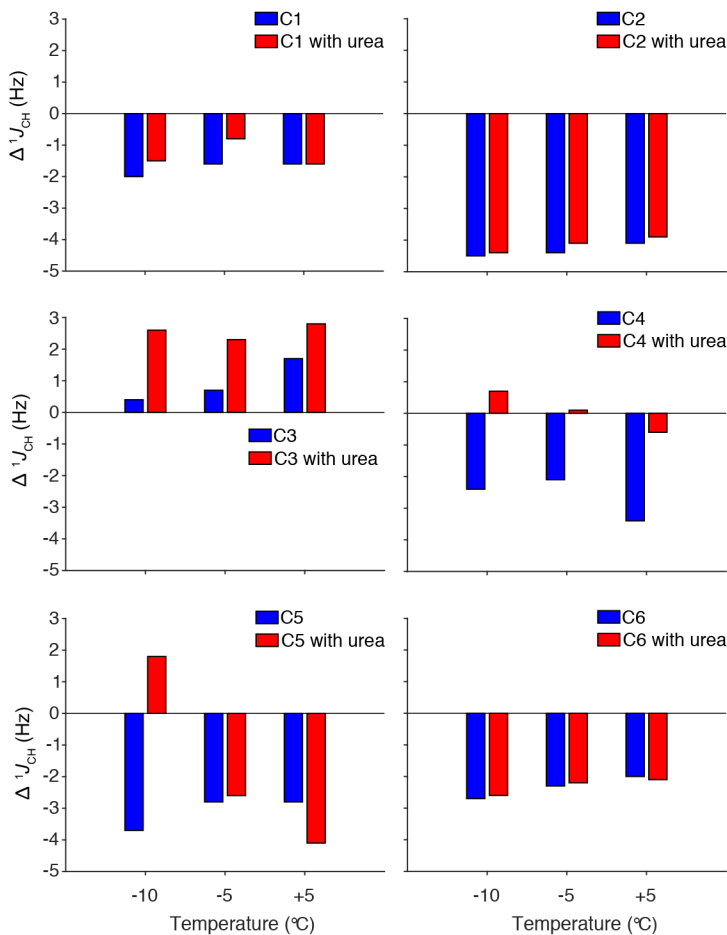


**Figure 6.3:** Difference in  $^1J_{CH}$  couplings of  $\beta$ -MeO-Glcp when dissolved in NaOH(aq) (blue) or NaOH(aq) with urea (red) in comparison to NaCl(aq) or NaCl(aq) with urea, respectively, for each temperature. All measurements were recorded in  $D_2O$ .

The difference in  $^1J_{CH}$  coupling was found to be equal for positions C1 and C6 at all temperatures and in the presence of urea, which might be an effect of

the solvent change from NaCl(aq) to NaOH(aq). Both positions C4 and C5 experienced a significant negative change in  $^1J_{CH}$  couplings in NaOH(aq), however, showing a different trend upon temperature increase:  $^1J_{CH}$  for C4 decreased further, while the trend was reversed for C5. Interestingly the addition of urea significantly affected these values, for C4 the  $^1J_{CH}$  observed upon dissolution in NaOH(aq) was dramatically reduced (only slight changes at -10 and +5°C could be observed), while for C5 the strong negative  $\Delta^1J_{CH}$  observed in NaOH(aq) turned into a positive value at -10°C.

Taken together, these results suggest that the  $^1J_{CH}$  couplings for  $\beta$ -MeO-Glcp are highly influenced by dissolution in NaOH(aq), but not strongly affected by a temperature variation. This indicates a conformational change or a possible exchange phenomenon, probably due to deprotonation. However, in the presence of urea in the NaOH(aq), the opposite was observed as conformational changes were induced by temperature, which affected positions C4 and C5.

### 6.3 Association of urea with a cellulose model compound

To further investigate the effect of urea in relation to the temperature dependency, a comparison of the  $^1J_{CH}$  coupling values +5°C with the values at -10°C in each of the solvents NaCl(aq) and NaOH(aq) upon the addition of urea was made (Figure 6.4).

In NaCl(aq), a significant temperature dependence was found for all positions except for C2 and the methyl group. Interestingly, upon the addition of urea to the NaCl(aq), the trend was reverted for positions C1, C3, and C5, which again suggests that urea itself is able to induce conformational changes in the  $\beta$ -MeO-Glcp. Position C5 exhibited the largest difference induced by the urea in NaCl(aq), which was -1.2 Hz. However, a different behaviour was observed in NaOH(aq), namely, positions C1, C2, and C6 revealed a more pronounced temperature dependence. Surprisingly, the effect of the temperature in NaCl(aq) on position C5 was reversed in NaOH(aq), going from an increase to a decrease in  $^1J_{CH}$  coupling. Even more remarkably, the effect on C5 was again reversed upon the addition of urea to the NaOH(aq), which clearly demonstrates the influence of urea on the chemical environment around position C5 and suggests an interaction between the  $\beta$ -MeO-Glcp and the urea.

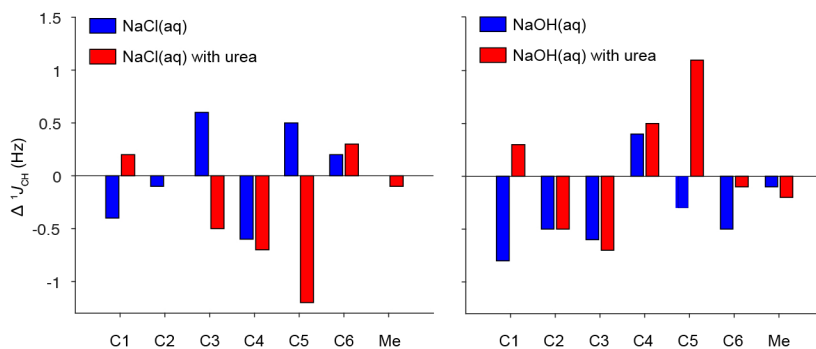


**Figure 6.4:** The change in  $^1J_{CH}$ -couplings of  $\beta$ -MeO-Glcp dissolved in NaCl(aq) or NaCl(aq) with urea and NaOH(aq) or NaOH(aq) with urea at +5 °C when compared to the  $^1J_{CH}$ -couplings at -10 °C. All measurements were recorded in D<sub>2</sub>O. Me corresponds to the methyl group on position C1.

To further examine this indicated interaction, a HOE experiment was performed on MCC dissolved in NaOH(aq) with the addition of  $^{15}\text{N}$ -labelled urea to monitor if magnetisation is transferred from the urea to the MCC, which would confirm a close and specific association between the two molecules. Indeed, the HOE experiment was able to confirm a close association as the intensity of the  $^1\text{H}$  spectrum of MCC increased upon the irradiation of the  $^{15}\text{N}$ -labelled urea (Figure 6.5). However, the increase was observed for all protons in the MCC, which, therefore, suggests the association to be non-specific. In other words, the urea appears to associate to all surfaces of the MCC and, hence, likely not accumulate on the more non-polar surfaces, which is in agreement with other studies.<sup>47,60</sup>

In conclusion, conformational changes in  $\beta$ -MeO-Glcp were induced by dissolution in NaOH(aq) but were not significantly affected by a variation in temperature in this solvent. However, a strong temperature dependence for the conformational changes of  $\beta$ -MeO-Glcp occurred in the presence of urea in the NaOH(aq). The non-specific association between urea and MCC suggests that the urea facilitates a more favourable chemical environment around the cellulose, inducing conformational changes, which can be one of the driving force for the improved dissolution of cellulose in NaOH(aq) upon the addition of urea. This is consistent with the work by Zhao et al.,<sup>57</sup> who reported on a change in the entropy of the system brought about by urea. Further, MD simulations re-



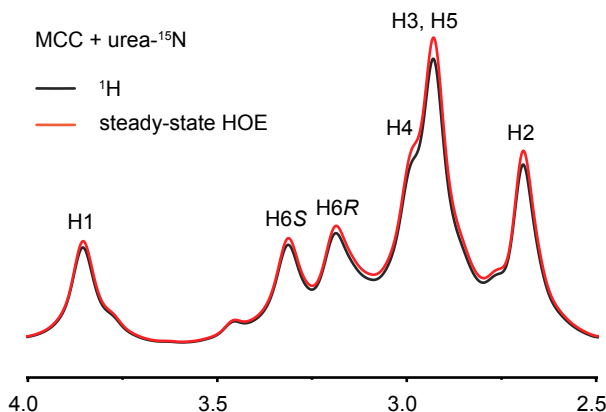


**Figure 6.5:** The steady-state HOE spectra of MCC dissolved in NaOH(aq) with urea- $^{15}\text{N}$ . All measurements were recorded at +5°C in  $\text{D}_2\text{O}$ .

ported by Wernersson et al.<sup>58</sup> show that urea itself, i.e. without the presence of NaOH, improves the solvent quality and favours interaction with the cellulose in solution. The addition of urea decreases the polarity of the solvent slightly, turning it into a more favourable solvent for a hydrophobic molecule to dissolve in. Hypothetically, the role of urea in NaOH(aq) could be to facilitate a more thermodynamically stable conformation of the amphiphilic polymer for the polar solvent to interact with, which aids dissolution. The thermodynamically stable conformation seems to be rather caused by the C-O rotation of the hydroxyl groups instead of a ring conformation because not all carbons revealed changes. Chen et al.<sup>83</sup> have studied the impact on dissolution of cellulose polymorphs in the presence of urea and concluded that the different conformations play an important role, which is in line with the results in the present thesis. Additionally, as our findings indicated an interaction, however a non-specific one, the urea is plausibly not very close and does not remain close to the cellulose for a longer period of time. Concerning the potential of urea to break hydrophobic interactions, close association of the urea to the hydrophobic patch does not agree with the results obtained from the HOESY experiment, but the theory cannot be ruled out as the association will be dependent on how the urea disrupts the hydrophobic interactions. Lastly, the results presented here do not agree with Egal et al.<sup>84</sup> who reported on the lack of difference in interactions between cellulose and NaOH(aq) in the presence or absence of urea.



# 7

## Molecular interactions in relation to CO<sub>2</sub> uptake in NaOH(aq)

*The sorption of CO<sub>2</sub> from air in NaOH(aq) leads to an unintentional addition of another solute in the solvent intended for the dissolution of cellulose, which impacts both the quality of the solvent and the molecular interactions in the system. Based on Papers I-IV, this chapter investigates and evaluates the effect of the addition of CO<sub>2</sub> to NaOH(aq), both prior to and after the dissolution of MCC or the cellulose model compounds  $\alpha$ -MeO-Glcp and  $\beta$ -MeO-Glcp.*

## 7.1 Influence on the chemical environment in NaOH(aq) by the addition of CO<sub>2</sub>

The inherent ability of NaOH(aq) to absorb CO<sub>2</sub> from the surrounding air is an overlooked feature of the dissolution of cellulose in NaOH(aq). The absorption of CO<sub>2</sub> consumes OH<sup>-</sup> ions in the conversion to CO<sub>3</sub><sup>2-</sup>, which affects the quality of the solvent due to the drop in pH. Studies on the reaction between deprotonated methanol in NaOH(aq) and added CO<sub>2</sub>(g)<sup>67</sup> suggest an additional feature of the cellulose/NaOH(aq) system as a possible reaction between deprotonated hydroxyl groups on cellulose and absorbed CO<sub>2</sub> from air that leads to the formation a cellulose carbonate. If this is true, the cellulose carbonate would then exist as a salt with Na<sup>+</sup> as a counterion. Upon regeneration of the cellulose solution, an anti-solvent is used to cause precipitation of the cellulose. This step is often performed through the addition of a neutralising agent, such as water or acid, causing hydrolysis of the carbonate. Ethanol, however, is known to preserve organic carbonates when used during the work-up of reactions in organic synthesis.<sup>85</sup>

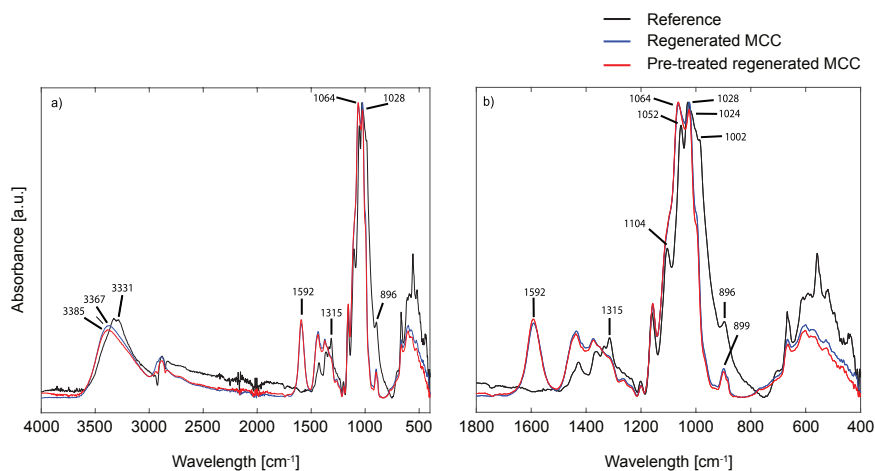


**Figure 7.1:** ATR-FTIR spectra from 4000-400 cm<sup>-1</sup> a) and zoomed in at 1800-400 cm<sup>-1</sup> b) for the reference MCC (black), MCC dissolved in NaOH(aq) and regenerated in ethanol (blue), and pre-treated MCC dissolved in NaOH(aq) and regenerated in ethanol (red).

Ethanol was, therefore, the choice of regenerating agent for the study of the proposed reaction between cellulose and CO<sub>2</sub>. To evaluate this, MCC (0.6 M)

dissolved in NaOH(aq) (2.0 M) was let to stand in contact with surrounding air for a fixed time before being regenerated and washed with ethanol. This step was followed by drying and analysis using ATR-IR spectroscopy. ATR-FTIR spectroscopy showed that the regenerated MCC had a new signature at  $1592\text{ cm}^{-1}$  in the spectrum when it was regenerated using ethanol (Figure 7.1 blue spectrum). This peak is known to correspond to an organic carbonate salt.<sup>86</sup> When using water as the regenerating agent, no peak at  $1592\text{ cm}^{-1}$  could be observed and hydrolysis plausibly occurred (see Fig. 4b) in the appended Paper I), which is commonly found for alkyl carbonate salts. The  $\text{CO}_2$  reaction was proven to be equally effective for untreated MCC as for MCC pre-treated with an organic superbases (see Paper I), which was expected to promote the interactions between MCC and  $\text{CO}_2$  (Figure 7.1 red spectrum). This result confirms that the reaction between MCC and  $\text{CO}_2$  occurs spontaneously in the NaOH(aq) solution.

In an attempt to investigate the observed incorporation of  $\text{CO}_2$  into dissolved cellulose *in-situ*, the model compound  $\alpha$ -MeO-Glcp (0.4 M) was chosen to obtain efficient dissolution in both a reference solvent (NaCl(aq)) and in the solvent of interest (NaOH(aq)).  $\text{CO}_2$ (g) was then added at a fixed rate before or after the dissolution of the  $\alpha$ -MeO-Glcp (pre or post-dissolution addition). The solutions were then analysed using  $^1\text{H}$  and  $^{13}\text{C}$  NMR spectroscopy. This experiment was expected to elucidate if the cellulose interacts with the  $\text{CO}_2$ (aq) or the  $\text{CO}_3^{2-}$  formed in the NaOH(aq). The formation of an organic carbonate would result in a new peak in the  $^{13}\text{C}$  NMR spectrum around 150 ppm but, surprisingly, such a peak was absent. Interestingly, the chemical shifts were affected differently depending on if the  $\text{CO}_2$  was added before or after the dissolution of  $\alpha$ -MeO-Glcp (see Fig. 4b) in the appended Paper II). The change in chemical shift is not surprising due to the known pH effect on the chemical shifts and the fact that the addition of  $\text{CO}_2$  decreases the pH of the solution. However, the addition of an equally large amount of  $\text{CO}_2$  should result in an equal change in chemical shifts if the change solely occurs due to the change in pH.

Similar results were found for the cellulose analogue  $\beta$ -MeO-Glcp upon the addition of  $\text{CO}_2$  before or after the dissolution in NaOH(aq) (Figure 7.2a)). It seems that, although a new peak corresponding to the formation of a new organic carbonate in the  $^{13}\text{C}$  NMR spectrum is absent, the time for the addition of the  $\text{CO}_2$  leads to a difference in the chemical environment for the cellulose model compound.

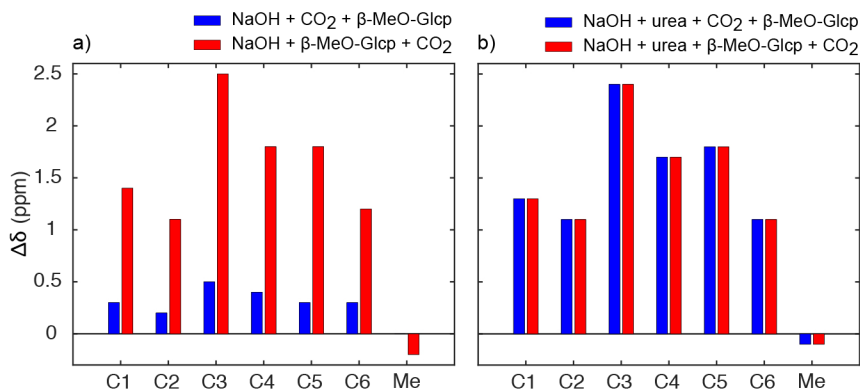


**Figure 7.2:** The change in chemical shift for all carbons in  $\beta$ -MeO-Glcp when dissolved in NaOH(aq) a) and NaOH(aq) with urea b) with pre or post-dissolution addition of CO<sub>2</sub>.

Further investigations of solutions containing urea (the most common additive in these systems) could provide additional valuable insights in the CO<sub>2</sub> chemistry of these solutions. Interestingly, in the presence of urea (2.5 M), the chemical shift change for the  $\beta$ -MeO-Glcp upon pre or post-dissolution addition of CO<sub>2</sub> vanished (Figure 7.2b)). In both cases, it was found that the change in chemical shift was equal, which suggests that when urea also is present, the same chemical environment is obtained for the  $\beta$ -MeO-Glcp regardless of when the CO<sub>2</sub> was added. In addition to this, a similar effect was found for the <sup>13</sup>C chemical shift value of the CO<sub>3</sub><sup>2-</sup>, which is generated in the reaction between CO<sub>2</sub> and OH<sup>-</sup> in the solvent (Table 7.1). The pre-dissolution addition of CO<sub>2</sub> resulted in the same chemical shift value for the CO<sub>3</sub><sup>2-</sup> as in pure NaOH(aq), i.e. the chemical environment for the CO<sub>3</sub><sup>2-</sup> was not affected by the presence of  $\beta$ -MeO-Glcp. However, the post-dissolution addition of CO<sub>2</sub> resulted in a decrease in chemical shift for the CO<sub>3</sub><sup>2-</sup>, which could indicate an interaction between the  $\beta$ -MeO-Glcp and CO<sub>3</sub><sup>2-</sup>. The same result was observed in system also containing urea. An analysis of the *J*<sub>HH</sub> coupling values for the  $\beta$ -MeO-Glcp in NaOH(aq) was also found to be in accordance. A conformational change occurred of the hydroxymethyl group upon post-dissolution addition of CO<sub>2</sub>, but was absent in the case of pre-dissolution addition. It appears that there is a difference in interaction between the two solutes if the  $\beta$ -MeO-Glcp is allowed to dissolve and, to a certain degree, become deprotonated prior to the addition of CO<sub>2</sub>. However, in the presence of urea, the conformational change was found to be equal both upon pre and post-dissolution addition of CO<sub>2</sub>. This equal change

in conformation is in line with finding of the chemical shift changes and that the presence of urea provides the same chemical environment for the  $\beta$ -MeO-Glcp regardless of when the  $\text{CO}_2$  is added. Interestingly, the chemical shift for the urea appeared to be unaffected by the addition of both  $\beta$ -MeO-Glcp and  $\text{CO}_2$ .

**Table 7.1:** *The  $^{13}\text{C}$  NMR chemical shifts in ppm of  $\text{CO}_3^{2-}$  and urea*

Sample	$\text{CO}_3^{2-}$	urea
NaOH + $\text{CO}_2$	171.1	-
NaOH + $\text{CO}_2$ + $\beta$ -MeO-Glcp	171.1	-
NaOH + $\beta$ -MeO-Glcp + $\text{CO}_2$	169.2	-
NaOH + urea + $\text{CO}_2$	171.1	165.6
NaOH + urea + $\text{CO}_2$ + $\beta$ -MeO-Glcp	170.9	165.5
NaOH + urea + $\beta$ -MeO-Glcp + $\text{CO}_2$	169.4	165.5

## 7.2 pH variation of NaOH(aq) induced by addition of different solutes

As pointed out in Section 7.1, the chemical shift values are sensitive to pH variations, which is why the pH of all the solutions was measured to understand on the origin of the difference in chemical shift values upon pre or post-dissolution addition of  $\text{CO}_2$  (Table 7.2). To compensate for the concentration and temperature dependency of the pH electrode, which only allows measurements up to pH 14, the solutions had to be diluted from 2.0 M to 0.5 M NaOH(aq) concentration. The results, however, show a relative comparison, which could provide valuable knowledge on the system. Information about the dynamics of the system containing NaOH(aq) or NaOH(aq) with urea can be obtained by comparing the change in pH that occurs depending on the order of the addition  $\text{CO}_2$  and  $\beta$ -MeO-Glcp.

From the pH measurements, both  $\alpha$ -MeO-Glcp and  $\beta$ -MeO-Glcp were found to be deprotonated in NaOH(aq) as the pH decreased by 0.09 and 0.18, respectively, upon dissolution in the NaOH(aq). It was found that the decrease in pH

occurred differently upon the pre or post-dissolution addition of  $\text{CO}_2$ . Pre and post-dissolution addition of  $\text{CO}_2$  to  $\alpha$ -MeO-Glcp solutions resulted in the same decrease in pH, which confirms that the difference in chemical shifts observed in Section 7.1 did not originate from a difference in the final pH of the two solutions. However, the pre or post-dissolution of  $\text{CO}_2$  with  $\beta$ -MeO-Glcp resulted in the same total decrease in pH, but the order of the addition of the  $\beta$ -MeO-Glcp and  $\text{CO}_2$  affected their individual decrease in pH differently. When  $\text{CO}_2$  was added to the solution before the  $\beta$ -MeO-Glcp, the decrease obtained was 0.44. In comparison, when  $\text{CO}_2$  instead was added after the dissolution of  $\beta$ -MeO-Glcp, the decrease in pH was 0.52. Due to the fact the total decrease in pH was equal for both pre and post-dissolution addition of  $\text{CO}_2$ , it is obvious that the  $\beta$ -MeO-Glcp also experienced different degree of deprotonation, depending on if  $\text{CO}_3^{2-}$  was present in the  $\text{NaOH(aq)}$  or not. The decrease in pH obtained with the dissolution of the  $\beta$ -MeO-Glcp in the presence of  $\text{CO}_3^{2-}$  (i.e. pre-dissolution addition of  $\text{CO}_2$ ) was found to be 0.31, while it was 0.18 when the  $\beta$ -MeO-Glcp was dissolved in the absence of  $\text{CO}_3^{2-}$  (i.e. post-dissolution addition of  $\text{CO}_2$ ). The same phenomenon was also observed upon the introduction of urea to the  $\text{NaOH(aq)}$ . From this examination it is suggested that the deprotonation of  $\beta$ -MeO-Glcp is promoted by the presence of  $\text{CO}_3^{2-}$  while the conversion of  $\text{CO}_2$  to  $\text{CO}_3^{2-}$  appears to be promoted by the presence of  $\beta$ -MeO-Glcp.

**Table 7.2:** *The difference in pH compared to the pH of  $\text{NaOH(aq)}$  (0.5 M) before the addition of  $\text{CO}_2$  (120 s) and MeO-Glcp. All measurements were made at +10°C*

Sample	$\Delta\text{pH}$ after addition of $\text{CO}_2$	$\Delta\text{pH}$ after addition of MeO-Glcp	Total $\Delta\text{pH}$
$\text{NaOH} + \text{CO}_2$	0.37	-	0.37
$\text{NaOH} + \text{CO}_2 + \alpha\text{-MeO-Glcp}$	0.37	0.09	0.46
$\text{NaOH} + \alpha\text{-MeO-Glcp} + \text{CO}_2$	0.36	0.08	0.44
$\text{NaOH} + \text{CO}_2$	0.44	-	0.44
$\text{NaOH} + \text{CO}_2 + \beta\text{-MeO-Glcp}$	0.44	0.31	0.75
$\text{NaOH} + \beta\text{-MeO-Glcp} + \text{CO}_2$	0.52	0.18	0.80
$\text{NaOH} + \text{urea} + \text{CO}_2$	0.15	-	0.15
$\text{NaOH} + \text{urea} + \text{CO}_2 + \beta\text{-MeO-Glcp}$	0.15	0.23	0.38
$\text{NaOH} + \text{urea} + \beta\text{-MeO-Glcp} + \text{CO}_2$	0.31	0.10	0.41



The presence of urea in the NaOH(aq) was found to result in an overall lower decrease in pH with the addition of CO<sub>2</sub>, which indicates that the urea acts as a buffering agent in the solution. In addition to this, a surprising observation was made initially when the urea was added to the pure NaOH(aq) and the pH increased from 13.90 to 14.00. The activity of the protons in the solution, which were measured with the pH electrode, seems to be restricted by the presence of urea. This phenomenon has been observed earlier by others.<sup>87–89</sup> In relation to the effect of urea on the conformational changes presented earlier, this reconfirmed finding clearly demonstrates that the NaOH(aq) as a solvent exhibits new features in the presence of urea, and that comparisons between the two solvents should be done with this in mind.

### 7.3 Catalytical capture of CO<sub>2</sub> in NaOH(aq) by MeO-Glcp and urea

The results reported by Faurholt<sup>67</sup> suggest that the addition of CO<sub>2</sub> to a solution of NaOH(aq) that contains an alcohol results in the formation of two products: an organic carbonate, from the reaction between the deprotonated alcohol and CO<sub>2</sub>; and CO<sub>3</sub><sup>2-</sup>, from the OH<sup>-</sup> and CO<sub>2</sub>. While the <sup>13</sup>C NMR measurements presented here showed a lack of an organic carbonate, an additional interesting feature of the CO<sub>3</sub><sup>2-</sup> peak was instead discovered. Upon integration of the CO<sub>3</sub><sup>2-</sup> peak, the post-dissolution addition of CO<sub>2</sub> to the solution containing dissolved  $\alpha$ -MeO-Glcp was found to be equal to more than twice the amount of CO<sub>3</sub><sup>2-</sup> in comparison to the CO<sub>3</sub><sup>2-</sup> peak in the pure NaOH(aq) solvent (Figure 7.3). The pre-dissolution addition of CO<sub>2</sub> was found to increase the uptake of CO<sub>2</sub> slightly more than the pure NaOH(aq) system.

Capturing of more than twice as much CO<sub>2</sub> with the post-dissolution addition of CO<sub>2</sub> should result in a much larger decrease in pH if the conversion to CO<sub>3</sub><sup>2-</sup> solely proceeds *via* the reaction with OH<sup>-</sup>. However, since the pH measurements revealed an equal reduction by pre and post-dissolution addition of CO<sub>2</sub>, the role of the  $\alpha$ -MeO-Glcp was again revised. Based on the fact that changes in the chemical shift appeared different with the post-dissolution addition of CO<sub>2</sub>, a reaction for the conversion of CO<sub>2</sub> into CO<sub>3</sub><sup>2-</sup> *via* the  $\alpha$ -MeO-Glcp, which works in a catalytical cycle, is suggested (Figure 7.4). The deprotonated  $\alpha$ -MeO-Glcp reacts with the CO<sub>2</sub> and forms an intermediate, which is readily hydrolysed by the water present, thus, resulting in the lean conversion of CO<sub>2</sub> to CO<sub>3</sub><sup>2-</sup> and the  $\alpha$ -MeO-Glcp proceeding in the catalytical cycle.

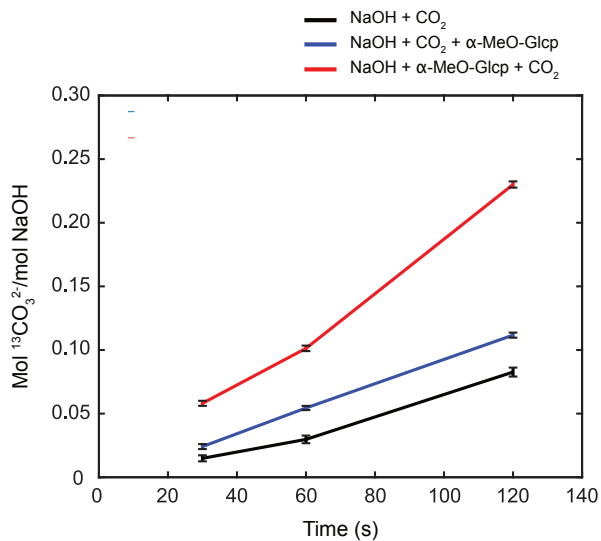


**Figure 7.3:** The uptake of CO<sub>2</sub> in NaOH(aq) (3.0 M) before or after the dissolution of α-MeO-Glcp as a function of time.

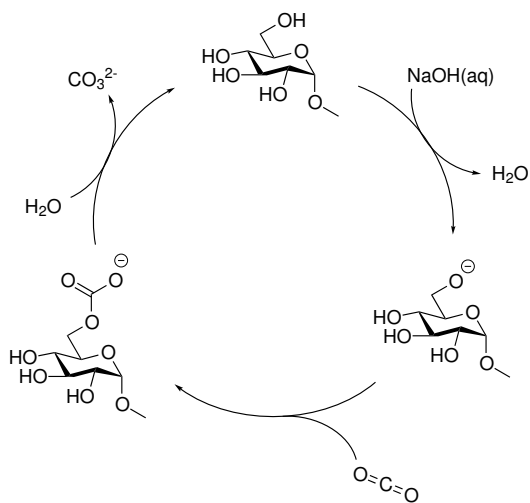


**Figure 7.4:** A proposed mechanism for the uptake of CO<sub>2</sub> in NaOH(aq) catalysed by α-MeO-Glcp.

While the *in-situ* study of the proposed reaction between  $\alpha$ -MeO-Glcp and  $\text{CO}_2$  was performed in  $\text{NaOH(aq)}$  at 3.0 M to ensure deprotonation, the succeeding study of the cellulose analogue  $\beta$ -MeO-Glcp was performed in the accurate conditions for cellulose dissolution in  $\text{NaOH(aq)}$ , namely, 2.0 M. The integration of the  $\text{CO}_3^{2-}$  peak in the system of 2.0 M  $\text{NaOH(aq)}$  and  $\beta$ -MeO-Glcp revealed the same phenomenon of an increased uptake of  $\text{CO}_2$  upon post-dissolution addition of  $\text{CO}_2$ . However, it also showed that even more  $\text{CO}_2$  was captured than in the 3.0 M system, which is probably due to a lower viscosity and, hence, increased reaction rates (Figure 7.5).

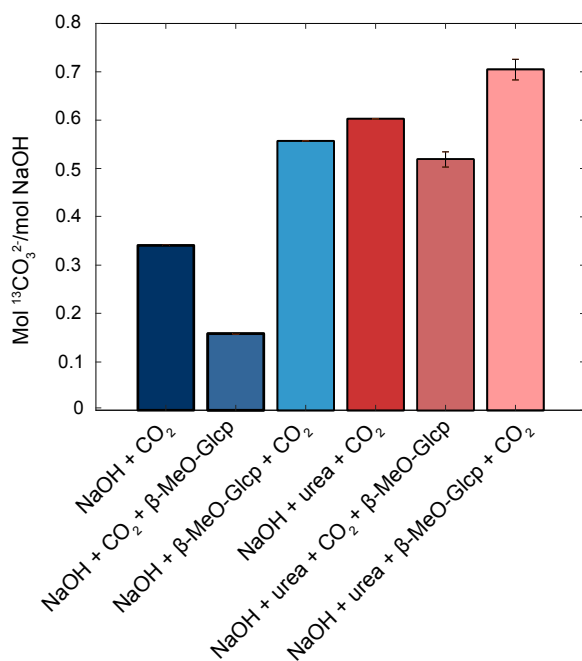


**Figure 7.5:** The uptake of  $\text{CO}_2$  in  $\text{NaOH(aq)}$  (2.0 M) and  $\text{NaOH(aq)}$  (2.0 M) with urea (2.5 M) before or after dissolution of  $\beta$ -MeO-Glcp.

Nonetheless, the opposite result was observed with the pre-dissolution addition of  $\text{CO}_2$ , as the uptake of  $\text{CO}_2$  appeared to be lower than for the pure  $\text{NaOH(aq)}$ . In contrast to the  $\alpha$ -analogue, the addition of  $\beta$ -MeO-Glcp to  $\text{NaOH(aq)}$  already containing  $\text{CO}_3^{2-}$  apparently decreases the amount of measurable  $\text{CO}_3^{2-}$ , which could indicate the precipitation of  $\text{Na}_2\text{CO}_3$ . The precipitation is then expected to be caused by the addition of the  $\beta$ -MeO-Glcp, although this

was not visible to the eye. Relating this phenomenon back to the observed drop in pH, depending on the order of addition of the different solutes, it appears that different chemical environments are generated if the  $\text{CO}_2$  is allowed to react into  $\text{CO}_3^{2-}$  *via* the cellulose model compounds or the  $\text{OH}^-$ , which is reflected in the changes in chemical shift for both the cellulose model compounds and  $\text{CO}_3^{2-}$ .

The introduction of urea in the solutions with pre or post-dissolution addition of  $\text{CO}_2$  in the presence of  $\beta$ -MeO-Glcp was also evaluated in terms of  $\text{CO}_2$  capture. In this study, it was found that the urea itself increased the amount of captured  $\text{CO}_2$  in the pure  $\text{NaOH(aq)}$ , which means that the urea contributes to the conversion of  $\text{CO}_2$  to  $\text{CO}_3^{2-}$  plausibly in a catalytical way since the  $^{13}\text{C}$  NMR spectroscopy did not reveal formation of new products in the system. However, the mechanism for this has not yet been investigated in this system. Again, the pre-dissolution addition of  $\text{CO}_2$  revealed a decrease in the amount of converted  $\text{CO}_2$ , while the post-dissolution addition of  $\text{CO}_2$  resulted in even higher capture of  $\text{CO}_2$  by the presence of both urea and  $\beta$ -MeO-Glcp. Thus, the catalytical role of both the urea and the  $\beta$ -MeO-Glcp did not seem to be disrupted by the presence of either solute.

#### 7.4 Is there association between $\text{CO}_3^{2-}$ and cellulose?

To further examine the indicated interaction between the cellulose model compound  $\beta$ -MeO-Glcp and  $\text{CO}_3^{2-}$  in the absence and presence of urea, a HOE experiment was performed on the system of MCC and  $^{13}\text{CO}_3^{2-}$  when dissolved in  $\text{NaOH(aq)}$  or  $\text{NaOH(aq)}$  with urea. A close association between the MCC and  $^{13}\text{CO}_3^{2-}$  results in a change in the  $^1\text{H}$  spectrum of the MCC due to MT from the  $^{13}\text{CO}_3^{2-}$ . The MT occurs when the  $^{13}\text{CO}_3^{2-}$  is irradiated prior to the recording of the  $^1\text{H}$  spectrum of the MCC and is evaluated by the comparison with a non-irradiated  $^1\text{H}$  spectrum.

In the system of  $\text{NaOH(aq)}$  with MCC and  $^{13}\text{CO}_3^{2-}$ , a decrease in signal intensity was found for all  $^1\text{H}$ 's in MCC, which demonstrates a non-specific interaction between the MCC and  $^{13}\text{CO}_3^{2-}$  (Figure 7.6). Important to mention, though, is that this experimental setup corresponds to the pre-dissolution addition of  $\text{CO}_2$  because  $^{13}\text{CO}_3^{2-}$  was dissolved together with the MCC and not added after the dissolution of MCC. The observed interaction between MCC and  $^{13}\text{CO}_3^{2-}$  is, however, an important sign of the preferred association between the

two solutes and supports the hypothesis of the formation of different chemical environments, depending on the order of addition of the two solutes. Interestingly, in the presence of urea, the previously observed interaction between the MCC and  $^{13}\text{CO}_3^{2-}$  was absent, which suggests that the urea either associate with the  $^{13}\text{CO}_3^{2-}$  or with the MCC, hence, disrupting and breaking the previously observed interaction. In other words, the association between  $\text{CO}_3^{2-}$  and urea is plausibly stronger than the interaction between  $\text{CO}_3^{2-}$  and MCC.

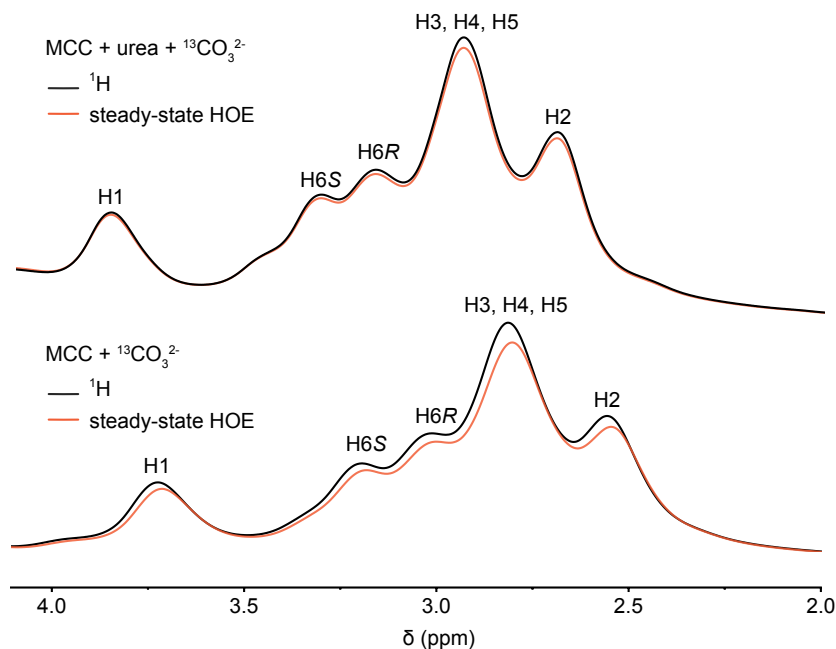


**Figure 7.6:** The steady-state HOE spectra of MCC dissolved in  $\text{NaOH(aq)}$  with  $^{13}\text{CO}_3^{2-}$  (bottom) and MCC dissolved in  $\text{NaOH(aq)}$  with urea and  $^{13}\text{CO}_3^{2-}$ . All measurements were recorded at  $+5^\circ\text{C}$ .

While an association between urea and  $\text{CO}_3^{2-}$  was not possible to observe in the  $^{13}\text{C}$  chemical shift values, ATR-FTIR spectroscopy on MCC dissolved in  $\text{NaOH(aq)}$  with urea and the addition of  $\text{CO}_2$  followed by precipitation in ethanol was able to indicate differently. The addition of  $\text{CO}_2$  both before and after the dissolution of cellulose in  $\text{NaOH(aq)}$  with urea gave rise to a new feature in the spectra. A peak appeared around  $1655\text{ cm}^{-1}$ , while the peak at  $1590\text{ cm}^{-1}$ , previously assigned to the cellulose carbonate, decreased (Figure 7.7). The fact

that neat urea has a strong signature at  $1590\text{ cm}^{-1}$  that is suppressed by the addition of  $\text{CO}_2$  suggests that there is a preferred association between the urea and the  $\text{CO}_3^{2-}$ . The observation of the counteracted interaction between MCC and  $\text{CO}_3^{2-}$  by urea (HOESY) falls in line with this. Formation of urea complexes has previously been reported as a change of the urea peaks at  $1677\text{ cm}^{-1}$  and  $1625\text{ cm}^{-1}$  to lower and higher wavenumber, respectively.<sup>90,91</sup> The peak at  $1655\text{ cm}^{-1}$  in the spectra at the top of Figure 7.7 could, therefore, be the result of the same change of the original urea peaks due to interaction with  $\text{CO}_3^{2-}$  in the system.

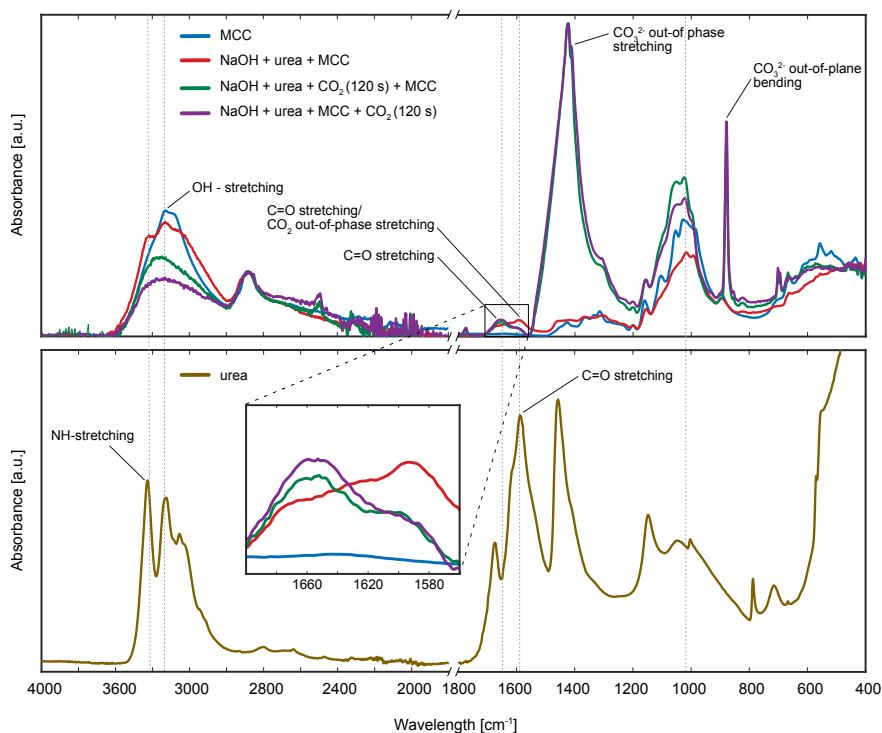


**Figure 7.7:** ATR-IR spectra from  $4000\text{--}400\text{ cm}^{-1}$ , at the top, of untreated MCC (blue) and MCC dissolved in  $\text{NaOH(aq)}$  + urea (red), MCC dissolved in  $\text{NaOH(aq)}$  + urea + pre-dissolution addition of  $\text{CO}_2$  (green) and MCC dissolved in  $\text{NaOH(aq)}$  + urea + post-dissolution addition of  $\text{CO}_2$  (purple). All solutions were precipitated in ethanol, washed until neutral and dried. ATR-IR spectrum from  $4000\text{--}400\text{ cm}^{-1}$ , at the bottom, of neat urea (brown) for comparison.

The effect of CO<sub>2</sub>, both with and without urea, on the dissolved cellulose in NaOH(aq) was further evaluated with the use of both static and dynamic light scattering in order to gain additional insight into the macromolecular features of the system. Samples were prepared by dissolving MCC (0.006 M) in NaOH(aq) (2.0 M) at -5°C, with or without the addition of urea (2.5 M), and with the pre or post-dissolution addition of CO<sub>2</sub> at a fixed rate. The method, as such, requires purification of the samples to remove dust and other scattering particle, and for this reason, the samples were filtered prior to the analysis. Unfortunately, the measurements were not to be repeatable, plausibly due to heavily varying filtration results.

In summary, the uptake of CO<sub>2</sub> in NaOH(aq) and its implication for molecular interactions in the solution occurs differently in the absence and presence of both a cellulose model compound/MCC and urea. From a cellulose dissolution point of view, it is apparent that the absorption of CO<sub>2</sub> in NaOH(aq) not only interferes with the quality of the solvent through the consumption of OH<sup>-</sup> and, hence, a decrease in pH, but also interferes with the molecular interactions between the solvent and the cellulose. The association between cellulose and CO<sub>3</sub><sup>2-</sup> occurs differently, depending on which solute is added first to the NaOH(aq). If a cellulose model compound is added first, more than twice as much CO<sub>2</sub> is captured than with a pure NaOH(aq) solution. This incorporation of CO<sub>2</sub> into the system occurs likely through the formation of a transient cellulose carbonate intermediate, which is readily hydrolysed to CO<sub>3</sub><sup>2-</sup> and water. The ability of a cellulose model compound to aid the capture of CO<sub>2</sub> could explain the spontaneous gelation of a cellulose/NaOH(aq) solution, where the increasing amount of CO<sub>3</sub><sup>2-</sup> could eventually lead to a significant decrease in pH or the formation of precipitated Na<sub>2</sub>CO<sub>3</sub>, which could work as precipitation nodes and cause to aggregation of the cellulose chains. In the presence of urea, the uptake of CO<sub>2</sub> is even larger, but the preferred interaction between CO<sub>3</sub><sup>2-</sup> and urea, compared to the interaction between CO<sub>3</sub><sup>2-</sup> and MCC, could be the reason for the prevented gelation of cellulose/NaOH(aq) in the presence of urea.

Taken together, the accessibility of a NaOH(aq) solution to the CO<sub>2</sub> present in the surrounding air could be an important parameter to control in the implementation of a NaOH(aq) process for the dissolution and regeneration of cellulose, e.g. for textile fibres. This is because the formation of CO<sub>3</sub><sup>2-</sup> could cause both interference in the molecular interactions during the dissolution as well as instability in the solution after dissolution has been achieved.





# 8

## Conclusions

*The studies included in this thesis have resulted in several findings that provide new insight into the process of dissolving cellulose in NaOH(aq). In this chapter, the findings are summarised and discussed in relation to each other. How these findings impact the dissolution of cellulose in NaOH(aq) is also discussed.*

## Scientific impact of the results

The results obtained from the experimental studies of this thesis show that cellulose dissolved in NaOH(aq) captures CO<sub>2</sub> from the ambient air in a catalytical route, which leads to a saturation of the system that, with time, will likely cause cellulose to gel and precipitate. This is possibly due to a close, but non-specific, association between the CO<sub>3</sub><sup>2-</sup> formed and the cellulose. Even more CO<sub>2</sub> is captured when urea is present in the system, but the formed CO<sub>3</sub><sup>2-</sup> possibly prefers to associate with the urea instead of the cellulose. Urea associates close, but in a non-specific manner, to cellulose, most likely to provide a more favourable chemical environment for the cellulose to dissolve in. The water dynamics in different aqueous alkali hydroxides and with the addition of urea, monitored with MT, were different and could be a contributing factor to the difference in the dissolution capacity of the different aqueous alkali solvents.

## Industrial impact of the results

From an industrial perspective the results obtained from the experiments in the thesis stress the importance of controlling the access of cellulose/NaOH(aq) solutions to air, CO<sub>2</sub>(g) in particular, during processing, as this will decrease the quality of the solution prior to regeneration. The cellulose not only exhibits alterations in its chemical environment when reacting with CO<sub>2</sub> but also catalyses the conversion of CO<sub>2</sub> to CO<sub>3</sub><sup>2-</sup>. In other words, the presence of CO<sub>3</sub><sup>2-</sup> in the system not only interferes with the cellulose chains but also creates in-balance in the chemistry of the system, which is possibly important control in the subsequent precipitation step.

In detail, the conclusions from each study can be summarised accordingly:

- MT provides a non-destructive tool for monitoring and investigating the swelling and dissolution of cellulose in different solvents.
- Conformational changes in  $\beta$ -MeO-Glcp occur in NaOH(aq), but are not strongly influenced by temperature variations.
- Urea associates to cellulose in a non-specific manner, which suggests that it interacts with cellulose indirectly by inducing changes in the chemical environment, which, in turn, induces conformational changes that make the polymer more prone to dissolve in NaOH(aq).
- $\text{CO}_2$  dissolves readily in NaOH(aq) and, in parallel with the  $\text{OH}^-$  mediated conversion to  $\text{CO}_3^{2-}$ , reacts with deprotonated cellulose, which forms an intermediate cellulose carbonate that is readily hydrolysed by water yielding  $\text{CO}_3^{2-}$ .
- The  $\text{CO}_3^{2-}$  formed in NaOH(aq) solutions containing a cellulose analogue shows different interactions with the carbohydrate depending on when (relative to the carbohydrate) it is introduced. When the  $\text{CO}_3^{2-}$  is present in the solution prior to the addition of the carbohydrate it seems to facilitate deprotonation of the incoming carbohydrate. Oppositely, when the  $\text{CO}_3^{2-}$  is formed through the addition of  $\text{CO}_2$  to a system containing already dissolved carbohydrate, the  $\text{CO}_3^{2-}$  seems to be stabilised by the very presence of the carbohydrate. This stabilisation is most likely promoted by a specific reaction between  $\text{CO}_2$ (aq) and carbohydrate alkoxides, which leads to a significantly higher incorporation of  $\text{CO}_3^{2-}$  into the solutions.
- In a NaOH(aq) solution containing cellulose and  $\text{CO}_3^{2-}$ , the  $\text{CO}_3^{2-}$  is associated non-specifically to the cellulose. The association between  $\text{CO}_3^{2-}$  and cellulose is counteracted by urea, which suggests that the  $\text{CO}_3^{2-}$  is more prone to associate to urea.



# 9

## Outlook

*From the findings in this thesis, additional research questions have arisen, which, in this chapter, are presented and formulated in terms of how specific investigations and methods can contribute to the knowledge on the dissolution mechanism for cellulose in NaOH(aq) and its peculiarities.*

To further evaluate and complement the findings of this thesis, a couple of future studies have been identified accordingly:

- To monitor the water dynamics that occur during the dissolution of cellulose, the parameters in the MT experiments need to be adjusted. The  $B_1$  frequency has to be tuned, and the  $T_1$ ,  $T_2$ , and  $T_1\rho$  parameters are important to re-evaluate in order to calculate the exchange between  $k_{\text{on}}$  and  $k_{\text{off}}$  for the water.
- MT should be recorded without cellulose in the solvent to control that the change or shape of the spectrum does not occur due to melting of the water or that hydrates are being formed.
- To be able to make a comparison with already published simulation data, the conformational changes induced by urea should be measured for the  $\beta$ -MeO-Glcp in a system only containing  $\text{D}_2\text{O}$  and urea, i.e. without addition of salt.
- The conformational changes in  $\beta$ -MeO-Glcp should be investigated also for other aqueous alkalis, with and without urea, and with varying temperature to examine and establish more information about the mechanism.
- $J$  couplings, using solid state NMR, could be interesting to measure on  $^{13}\text{C}$ -labelled sugar/cellulose or a  $^{13}\text{C}$  bred plant to evaluate if the change is true also for cellulose and compared with the values for  $\beta$ -MeO-Glcp in solution.
- The cellulose carbonate intermediate could possibly be observed with NMR spectroscopy using addition of  $^{13}\text{C}$ -labelled  $\text{CO}_2$  in the  $\text{NaOH}(\text{aq})$  solutions.
- The conversion of  $\text{CO}_2$  to  $\text{CO}_3^{2-}$ , which is suggested to occur *via* the urea, should be examined and studied in detail without the  $\beta$ -MeO-Glcp in the  $\text{NaOH}(\text{aq})$  system.
- The capture of  $\text{CO}_2$  in the  $\text{NaOH}(\text{aq})$ /cellulose system should also be evaluated with the addition of other known dissolution aiding additives, e.g.  $\text{ZnO}$  and thiourea to investigate how they influence the formation of  $\text{CO}_3^{2-}$ .

# Acknowledgements

Södra Skogsägarnas Stiftelse för Forskning, Utveckling och Utbildning is acknowledged for their financial support.

I would like to express my gratitude to my examiner **Hans Theliander**. Thanks for taking me in as a PhD student and for the support during the years.

To my supervisor **Merima Hasani**. Thanks for all our fruitful discussions regarding chemistry, academia or just life in general. Best of luck with lifting our CO<sub>2</sub>-findings to the next level!

A special thanks to my co-supervisor, **Diana Bernin** for showing me the beauty of NMR, and for always being there for me when research and life are troublesome!

Extra thanks to my co-supervisor and mentor **Gunnar Westman** for your never failing encouragement and for always guiding me in the right direction.

Thanks to **all my scientific colleagues, Malin Larsson, and Ximena Rozo Sevilla** at Forest Products and Chemical Engineering, and to all colleagues within **the Avancell network**.

I would also like to thank **my new colleagues at RISE**, and especially **Åsa Östlund, Hanna de la Motte, and Malin Viola Wennberg** for giving me the opportunity to experience when fashion and chemistry come together. Keep up the good work!

Big thanks to the ladies **Rebbe, Ida, Eve, Kim, Nina, Anna, Lisa, and many more** for bringing glitter and dance into my life! Your guys are OK as well!

Thanks to all great friends **Nenne, Jenny, Jenny, Artur, Jesper, Emil, Maria, Johan, Mattias, Alex, and Carina**.

My endless love to **my parents** for always believing in me and for supporting me and my family through everything in life.

Last but not least, **Frank and Pontus** I love you! ♥





# Bibliography

- (1) The Fiber Year. The Fiber Year 2018., 2018.
- (2) Chapagain, A. K.; Hoekstra, A. Y.; Savenije, H. H. G.; Gautam, R. The water footprint of cotton consumption: An assessment of the impact of world-wide consumption of cotton products on the water resources in the cotton producing countries. *Ecol. Econ.* **2006**, *60*, 186–203.
- (3) Tariq, M. I.; Afzal, S.; Hussain, I.; Sultana, N. Pesticides exposure in Pakistan: a review. *Environ. Int.* **2007**, *33*, 1107–1122.
- (4) Budtova, T.; Navard, P. Cellulose in NaOH–water based solvents: a review. *Cellulose* **2016**, *23*, 5–55.
- (5) French, A. D. Glucose, not cellobiose, is the repeating unit of cellulose and why that is important. *Cellulose* **2017**, *24*, 4605–4609.
- (6) Jr, R. B.; Saxena, I. M. Cellulose biosynthesis: A model for understanding the assembly of biopolymers. *Plant Physiol. Biochem.* **2000**, *38*, 57–67.
- (7) Jarvis, M. C. Cellulose Biosynthesis: Counting the Chains. *Plant Physiol.* **2013**, *163*, 1485–1486.
- (8) Nixon, B. T.; Mansouri, K.; Singh, A.; Du, J.; Davis, J. K.; Lee, J.-G.; Slabaugh, E.; Vandavasi, V. G.; O'Neill, H.; Roberts, E. M.; Roberts, A. W.; Yingling, Y. G.; Haigler, C. H. Comparative Structural and Computational Analysis Supports Eighteen Cellulose Synthases in the Plant Cellulose Synthesis Complex. *Sci. Rep.* **2016**, *6*, 28696.
- (9) Nishiyama, Y.; Sugiyama, J.; Chanzy, H.; Langan, P. Crystal Structure and Hydrogen Bonding System in Cellulose Ia from Synchrotron X-ray and Neutron Fiber Diffraction. *J. Am. Chem. Soc.* **2003**, *125*, 14300–14306.
- (10) Lindman, B.; Karlström, G.; Stigsson, L. On the mechanism of dissolution of cellulose. *J. Mol. Liq.* **2010**, *156*, 76–81.

- (11) Sixta, H., *Handbook of pulp*. Wiley-VCH: 2006.
- (12) Rockwell, G. D.; Grindley, T. B. Effect of Solvation on the Rotation of Hydroxymethyl Groups in Carbohydrates. *J. Am. Chem. Soc.* **1998**, *120*, 10953–10963.
- (13) Stenutz, R.; Carmichael, I.; Widmalm, G.; Serianni, A. S. Hydroxymethyl Group Conformation in Saccharides: Structural Dependencies of  $^2J_{\text{HH}}$ ,  $^3J_{\text{HH}}$ , and  $^1J_{\text{CH}}$  Spin-Spin Coupling Constants. *J. Org. Chem.* **2002**, *67*, 949–958.
- (14) Angles d'Ortoli, T.; Sjöberg, N. A.; Vasiljeva, P.; Lindman, J.; Widmalm, G.; Bergenstråhle-Wohlert, M.; Wohlert, J. Temperature Dependence of Hydroxymethyl Group Rotamer Populations in Cellooligomers. *J. Phys. Chem. B* **2015**, *119*, 9559–9570.
- (15) Atalla, R. H.; Vanderhart, D. L. Native Cellulose: A Composite of Two Distinct Crystalline Forms. *Science* **1984**, *223*, 283–285.
- (16) O'Sullivan, A. Cellulose: the structure slowly unravels. *Cellulose* **1997**, *4*, 173–207.
- (17) Langan, P.; Nishiyama, Y.; Chanzy, H. X-ray Structure of Mercerized Cellulose II at 1 Å Resolution. *Biomacromolecules* **2001**, *2*, 410–416.
- (18) Kolpak, F. J.; Weih, M.; Blackwell, J. Mercerization of cellulose: 1. Determination of the structure of Mercerized cotton. *Polymer* **1978**, *19*, 123–131.
- (19) Zugenmaier, P. In *Crystalline Cellulose and Derivatives: Characterization and Structures*, Timell, T. E., Wimmer, R., Eds.; Springer-Verlag: Heidelberg, 2008, pp. 101–174.
- (20) Glasser, W.; Atalla, R.; Blackwell, J.; Malcolm Brown Jr., R.; Burchard, W.; French, A.; Klemm, D.; Nishiyama, Y. About the structure of cellulose: debating the Lindman hypothesis. *Cellulose* **2012**, *19*, 589–598.
- (21) Heinze, T.; Koschella, A. Solvents applied in the field of cellulose chemistry: a mini review. *Polímeros* **2005**, *15*, 84–90.
- (22) Lindman, B.; Medronho, B.; Alves, L.; Costa, C.; Edlund, H.; Norgren, M. The relevance of structural features of cellulose and its interactions to dissolution, regeneration, gelation and plasticization phenomena. *Phys. Chem. Chem. Phys.* **2017**, 23704–23718.
- (23) Medronho, B.; Lindman, B. Competing forces during cellulose dissolution: From solvents to mechanisms. *Curr. Opin. Colloid Interface Sci.* **2014**, *19*, 32–40.

- (24) Jiang, Z.; Fang, Y.; Ma, Y.; Liu, M.; Liu, R.; Guo, H.; Lu, A.; Zhang, L. Dissolution and Metastable Solution of Cellulose in NaOH/Thiourea at 8°C for Construction of Nanofibers. *J. Phys. Chem. B* **2017**, *121*, 1793–1801.
- (25) Qi, H.; Yang, Q.; Zhang, L.; Liebert, T.; Heinze, T. The dissolution of cellulose in NaOH-based aqueous system by two-step process. *Cellulose* **2011**, *18*, 237–245.
- (26) Luo, X.; Zhang, L. New solvents and functional materials prepared from cellulose solutions in alkali/urea aqueous system. *Food Res. Int.* **2013**, *52*, 387–400.
- (27) Alves, L.; Medronho, B.; Antunes, F. E.; Topgaard, D.; Lindman, B. Dissolution state of cellulose in aqueous systems. 1. Alkaline solvents. *Cellulose* **2016**, *23*, 247–258.
- (28) Alves, L.; Medronho, B.; Antunes, F. E.; Topgaard, D.; Lindman, B. Dissolution state of cellulose in aqueous systems. 2. Acidic solvents. *Carbohydr. Polym.* **2016**, *151*, 707–715.
- (29) Sixta, H.; Michud, A.; Hauru, L.; Asaadi, S.; Ma, Y.; King, A. W.; Kilpeläinen, I.; Hummel, M. Ioncell-F: A High-strength regenerated cellulose fibre. *Nord. Pulp Pap. Res. J.* **2015**, *30*, 43.
- (30) Lenzing AG Sustainability., 2019.
- (31) VTT The cellulose carbamate process., 2017.
- (32) Liebert, T. In *Cellulose Solvents: For Analysis, Shaping and Chemical Modification*, 2010; Chapter 1, pp. 3–54.
- (33) Yang, Y.; Xie, H.; Liu, E. Acylation of cellulose in reversible ionic liquids. *Green Chem.* **2014**, *16*, 3018–3023.
- (34) Cuissinat, C.; Navard, P. Swelling and Dissolution of Cellulose Part 1: Free Floating Cotton and Wood Fibres in N-Methylmorpholine-N-oxide-Water Mixtures. *Macromol. Symp.* **2006**, *244*, 1–18.
- (35) Graenacher, C. Cellulose solution. US 1943176A., 1934.
- (36) Swatloski, R. P.; Spear, S. K.; Holbrey, J. D.; Rogers, R. D. Dissolution of Cellulose with Ionic Liquids. *J. Am. Chem. Soc.* **2002**, *124*, 4974–4975.
- (37) Zheng, W.; Mohammed, A.; Hines, L. G.; Xiao, D.; Martinez, O. J.; Bartsch, R. A.; Simon, S. L.; Russina, O.; Triolo, A.; Quitevis, E. L. Effect of Cation Symmetry on the Morphology and Physicochemical Properties of Imidazolium Ionic Liquids. *J. Phys. Chem. B* **2011**, *115*, 6572–6584.

- (38) The London Journal and Repertory of Arts and Science Specification of a patent granted to John Mercer, of Oakenshaw, Lancashire, for improvements in the preparation of cotton and other fabrics and fibrous materials. [Sealed 24<sup>th</sup> October, 1850]. *J. Franklin Inst.* **1851**, 52, 202–204.
- (39) Woodings, C. The viscose process., 2001.
- (40) Lilienfeld, L. Manufacture of Cellulose solution. British patent no. 212864., 1924.
- (41) Davidson, G. F. The dissolution of chemically modified cotton cellulose in alkaline solutions. Part I - In solutions of sodium hydroxide, particularly at temperatures below the normal. *J. Text. Inst. Trans.* **1934**, 25, T174–T196.
- (42) Sobue, H.; Kiessig, H.; Hess, K. The system: cellulose-sodium hydroxide-water in relation to the temperature. *Z. Physik Chem B.* **1939**, 43, 309–328.
- (43) Yamashiki, T.; Kamide, K.; Okajima, K.; Kowsaka, K.; Matsui, T.; Fukase, H. Some Characteristic Features of Dilute Aqueous Alkali Solutions of Specific Alkali Concentration (2.5 mol l<sup>-1</sup>) Which Possess Maximum Solubility Power against Cellulose. *Polym J* **1988**, 20, 447–457.
- (44) Marsh, J., *Mercerising*; Chapman & Hall: London, 1941.
- (45) Xiong, B.; Zhao, P.; Cai, P.; Zhang, L.; Hu, K.; Cheng, G. NMR spectroscopic studies on the mechanism of cellulose dissolution in alkali solutions. *Cellulose* **2013**, 20, 613–621.
- (46) Roy, C.; Budtova, T.; Navard, P.; Bedue, O. Structure of Cellulose-Soda Solutions at Low Temperatures. *Biomacromolecules* **2001**, 2, 687–693.
- (47) Egal, M.; Budtova, T.; Navard, P. Structure of Aqueous Solutions of Micro-crystalline Cellulose/Sodium Hydroxide below 0°C and the Limit of Cellulose Dissolution. *Biomacromolecules* **2007**, 8, 2282–2287.
- (48) Kamide, K.; Okajima, K.; Kowsaka, K. Dissolution of Natural Cellulose into Aqueous Alkali Solution: Role of Super-Molecular Structure of Cellulose. *Polym. J.* **1992**, 24, 71–86.
- (49) Isogai, A. NMR analysis of cellulose dissolved in aqueous NaOH solutions. *Cellulose* **1997**, 4, 99–107.
- (50) Bialik, E.; Stenqvist, B.; Fang, Y.; Östlund, Å.; Furó, I.; Lindman, B.; Lund, M.; Bernin, D. Ionization of Cellobiose in Aqueous Alkali and the Mechanism of Cellulose Dissolution. *J. Phys. Chem. Lett.* **2016**, 7, 5044–5048.

- (51) Gubitosi, M.; Nosrati, P.; Koder Hamid, M.; Kuczera, S.; Behrens, M. A.; Johansson, E. G.; Olsson, U. Stable, metastable and unstable cellulose solutions. *R. Soc. Open Sci.* **2017**, *4*.
- (52) Klemm, D.; Philipp, B.; Heinze, T.; Heinze, U.; Wagenknecht, W. In *Comprehensive Cellulose Chemistry*; John Wiley & Sons, Ltd: 2004; Chapter 4.2.3-4.2. pp. 51–71.
- (53) Laszkiewicz, B.; Wcislo, P. Sodium cellulose formation by activation process. *J. Appl. Polym. Sci.* **1990**, *39*, 415–425.
- (54) Laszkiewicz, B. Solubility of bacterial cellulose and its structural properties. *J. Appl. Polym. Sci.* **1998**, *67*, 1871–1876.
- (55) Rossky, P. J. Protein denaturation by urea: Slash and bond. *Proc. Natl. Acad. Sci. U. S. A.* **2008**, *105*, 16825–16826.
- (56) Preston, J. M.; Clark, J. F.; Beath, W. R.; Nimkar, M. V. 31-Swelling Powers of Urea Solutions on Cellulose. *J. Text. Inst. Trans.* **1954**, *45*, T504–T509.
- (57) Zhao, Y.; Liu, X.; Wang, J.; Zhang, S. Effects of anionic structure on the dissolution of cellulose in ionic liquids revealed by molecular simulation. *Carbohydr. Polym.* **2013**, *94*, 723–730.
- (58) Wernersson, E.; Stenqvist, B.; Lund, M. The mechanism of cellulose solubilization by urea studied by molecular simulation. *Cellulose* **2015**, *22*, 991–1001.
- (59) Jiang, Z.; Fang, Y.; Xiang, J.; Ma, Y.; Lu, A.; Kang, H.; Huang, Y.; Guo, H.; Liu, R.; Zhang, L. Intermolecular Interactions and 3D Structure in Cellulose-NaOH/urea Aqueous System. *J. Phys. Chem. B* **2014**, *118*, 10250–10257.
- (60) Cai, J.; Zhang, L.; Liu, S.; Liu, Y.; Xu, X.; Chen, X.; Chu, B.; Guo, X.; Xu, J.; Cheng, H.; Han, C. C.; Kuga, S. Dynamic Self-Assembly Induced Rapid Dissolution of Cellulose at Low Temperatures. *Macromolecules* **2008**, *41*, 9345–9351.
- (61) Bergenstråhle-Wohlert, M.; Berglund, L. A.; Brady, J. W.; Larsson, P. T.; Westlund, P.-O.; Wohlert, J. Concentration enrichment of urea at cellulose surfaces: results from molecular dynamics simulations and NMR spectroscopy. *Cellulose* **2012**, *19*, 1–12.
- (62) Xiong, B.; Zhao, P.; Hu, K.; Zhang, L.; Cheng, G. Dissolution of cellulose in aqueous NaOH/urea solution: role of urea. *Cellulose* **2014**, *21*, 1183–1192.

- (63) Isobe, N.; Kimura, S.; Wada, M.; Kuga, S. Mechanism of cellulose gelation from aqueous alkali-urea solution. *Carbohydr. Polym.* **2012**, *89*, 1298–1300.
- (64) Zhang, L.; Ruan, D.; Gao, S. Dissolution and regeneration of cellulose in NaOH/thiourea aqueous solution. *J. Polym. Sci. Part B Polym. Phys.* **2002**, *40*, 1521–1529.
- (65) Davidson, G. F. The dissolution of chemically modified cotton cellulose in alkaline solutions. Part 3 - In solutions of sodium and potassium hydroxide containing dissolved zinc, beryllium and aluminium oxides. *J. Text. Inst. Trans.* **1937**, *28*, T27–T44.
- (66) Yang, Q.; Qi, H.; Lue, A.; Hu, K.; Cheng, G.; Zhang, L. Role of sodium zincate on cellulose dissolution in NaOH/urea aqueous solution at low temperature. *Carbohydr. Polym.* **2011**, *83*, 1185–1191.
- (67) Faurholt, C. Studies on monoalkyl carbonates. II. The formation of monoalkyl carbonic acids or their salts on dissolving carbon dioxide in aqueous solutions of alcohols of different degrees of acidity. *Z. Physik Chem B.* **1927**, *126*, 85–104.
- (68) Song, D.; Rochelle, G. T. Reaction kinetics of carbon dioxide and hydroxide in aqueous glycerol. *Chem. Eng. Sci.* **2017**, *161*, 151–158.
- (69) Lemieux, R. U. Effects of unshared pairs of electrons and their solvation on conformational equilibria. *Pure Appl. Chem.* **1971**, *25*, 527.
- (70) Cai, J.; Zhang, L. Unique Gelation Behavior of Cellulose in NaOH/Urea Aqueous Solution. *Biomacromolecules* **2005**, *7*, 183–189.
- (71) Washburn, E. W. In *International Critical Tables of Numerical Data, Physics, Chemistry and Technology (1st Electronic Edition)*; Knovel: 1926, 258:259.
- (72) Zaiss, M.; Zu, Z.; Xu, J.; Schuenke, P.; Gochberg, D. F.; Gore, J. C.; Ladd, M. E.; Bachert, P. A combined analytical solution for chemical exchange saturation transfer and semi-solid magnetization transfer. *NMR Biomed.* **2015**, *28*, 217–230.
- (73) Anthis, N. J.; Clore, G. M. Visualizing transient dark states by NMR spectroscopy. *Q. Rev. Biophys.* **2015**, *48*, 35–116.
- (74) Zhou, J.; van Zijl, P. C. M. Chemical exchange saturation transfer imaging and spectroscopy. *Prog. Nucl. Magn. Reson. Spectrosc.* **2006**, *48*, 109–136.

- (75) Sled, J. G. Modelling and interpretation of magnetization transfer imaging in the brain. *NeuroImage* **2018**, *182*, 128–135.
- (76) Roy, C.; Budtova, T.; Navard, P. Rheological Properties and Gelation of Aqueous Cellulose-NaOH Solutions. *Biomacromolecules* **2003**, *4*, 259–264.
- (77) Kamide, K.; Saito, M.; Kowsaka, K. Temperature Dependence of Limiting Viscosity Number and Radius of Gyration for Cellulose Dissolved in Aqueous 8% Sodium Hydroxide Solution. *Polym. J.* **1987**, *19*, 1173–1181.
- (78) Stenqvist, B.; Wernersson, E.; Lund, M. Cellulose-Water Interactions: Effect of electronic polarizability. *Nord. Pulp Pap. Res. J.* **2015**, *30*, 26.
- (79) Hadden, J. A.; French, A. D.; Woods, R. J. Unraveling Cellulose Microfibrils: A Twisted Tale. *Biopolymers* **2013**, *99*, 746–756.
- (80) Sivan, U. The inevitable accumulation of large ions and neutral molecules near hydrophobic surfaces and small ions near hydrophilic ones. *Curr. Opin. Colloid Interface Sci.* **2016**, *22*, 1–7.
- (81) Lindman, B.; Karlström, G. Nonionic polymers and surfactants: Temperature anomalies revisited. *Comptes Rendus Chim.* **2009**, *12*, 121–128.
- (82) Bergenstråhle-Wohlert, M.; Angles d'Ortoli, T.; Sjöberg, N. A.; Widmalm, G.; Wohlert, J. On the anomalous temperature dependence of cellulose aqueous solubility. *Cellulose* **2016**, *23*, 2375–2387.
- (83) Chen, X.; Jinghuan Chen; You, T.; Kun Wang; Xu, F. Effects of polymorphs on dissolution of cellulose in NaOH/urea aqueous solution. *Carbohydr. Polym.* **2015**, *125*, 85–91.
- (84) Egal, M.; Budtova, T.; Navard, P. The dissolution of microcrystalline cellulose in sodium hydroxide-urea aqueous solutions. *Cellulose* **2008**, *15*, 361–370.
- (85) Franchimont, A. P. N. On sodium-alkyl carbonates. *KNAW Proceedings* **1910**, *12*, 303–304.
- (86) Larkin, P.; Larkin, P. In *Infrared and Raman Spectroscopy*; Elsevier: Oxford, 2011, pp. 73–115.
- (87) Bull, H. B.; Breese, K.; Ferguson, G. L.; Swenson, C. A. The pH of urea solutions. *Arch. Biochem. Biophys.* **1964**, *104*, 297–304.
- (88) Schäfer, O. F. Effect of Urea on the Titration Behaviour of Acetic Acid. *Ber. Bunsenges. Phys. Chem.* **1976**, *80*, 529–532.

- (89) Das Gupta, P. K.; Moulik, S. P. Interaction of urea with weak acids and water. *J. Phys. Chem.* **1987**, *91*, 5826–5832.
- (90) Manivannan, M.; Rajendran, S. Investigation of inhibitive action of urea- $\text{Zn}^{2+}$  system in the corrosion control of carbon steel in sea water. *Int. J. Eng. Sci. Technol.* **2011**, *3*.
- (91) Gangopadhyay, D.; Singh, S. K.; Sharma, P.; Mishra, H.; Unnikrishnan, V. K.; Singh, B.; Singh, R. K. Spectroscopic and structural study of the newly synthesized heteroligand complex of copper with creatinine and urea. *Spectrochim. Acta Part A Mol. Biomol. Spectrosc.* **2016**, *154*, 200–206.